GEODYNAMICS & TECTONOPHYSICS

PUBLISHED BY THE INSTITUTE OF THE EARTH'S CRUST
SIBERIAN BRANCH OF RUSSIAN ACADEMY OF SCIENCES

2016 VOLUME 7 ISSUE 2 PAGES 143–172 ISSN 2078-502X

http://dx.doi.org/10.5800/GT-2016-7-2-0202

Paleogeodynamics

BONINITES THROUGH TIME AND SPACE: PETROGENESIS AND GEODYNAMIC SETTINGS

A. A. Shchipansky

Geological Institute of RAS, Moscow, Russia

Abstract: The article provides an overview of boninitic magmatism occurrences in space and time and shows that the boninite rock series were generated through the entire geological history of the Earth. In modern environments, the genesis of boninites is related to intra-oceanic subduction initiation. Boninites are typical members of suprasubduction zone ophiolite sequences in the Phanerozoic fold belts and also present in the early Precambrian greenstone belts. A comparative study on compositions of the early Precambrian and Phanerozoic boninites indicate their evolution through time due to gradual transition from the early thick-plate tectonics to the modern thin-plate tectonics. A link between subduction initiation and mantle-plume impingement at the oceanic lithosphere is discussed.

Key words: boninite; subduction initiation; mantle plume; secular changing in the Earth geodynamics

Recommended by E.V. Sklyarov

For citation: *Shchipansky A.A.* 2016. Boninites through time and space: petrogenesis and geodynamic settings. *Geodynamics & Tectonophysics* 7 (2), 143–172. doi:10.5800/GT-2016-7-2-0202.

БОНИНИТЫ ВО ВРЕМЕНИ И ПРОСТРАНСТВЕ: ПЕТРОГЕНЕЗИС И ГЕОДИНАМИЧЕСКИЕ ОБСТАНОВКИ ОБРАЗОВАНИЯ

А. А. Щипанский

Геологический институт РАН, Москва, Россия

Аннотация: Бониниты получили широкую известность благодаря глубоководным исследованиям преддуговых областей современных зон плитовой конвергенции Юго-Западной Пацифики. Однако они имеют широкое распространение и в офиолитах складчатых поясов, которые традиционно рассматриваются в качестве океанической коры геологического прошлого. Поскольку бониниты не известны в срединно-океанических хребтах, неизбежно возникает вопрос о природе офиолитов.

Общепринято, что под бонинитами понимаются вулканические породы, которые удовлетворяют следующим критическим параметрам составов (в пересчете на сухой остаток) – SiO_2>52 вес. %; MgO>8 вес. % и TiO_2<0.5 вес. % [*Le Bas, 2000*]. Их классификация основана на различиях в химических, а не минералогических составах, и принято различать две крупные группы бонинитов – высококальциевые и низкокальциевые [*Crawford et al., 1989*]. С бонинитами пространственно и генетически связаны примитивные островодужные низко-Ti лавы, что предопределило необходимость выделения обособленной магматической серии, известной как бонинитовая серия [*Pearce, Robinson, 2010*]. Собственно бониниты являются наиболее фракционированной ветвью серии, которая берет начало в пикритовых низко-Ti расплавах. Характер распределения спектра малых элементов бонинитов наглядно показывает необычайно высокую степень деплетации ман-

тийного источника при одновременных свидетельствах их надсубдукционного генезиса, например отрицательных аномалиях Nb(Ta) и Ti. Спектры малых элементов бонинитовой серии таковы, что, во-первых, исключается участие какого-либо вклада в их петрогенезис материала континентальной коры и, во-вторых, требуется плавление мантийного источника, более деплетированного по сравнению с лерцолитовой мантией, генерирующей расплавы MORB. В то же время геохимия пород бонинитовой серии демонстрирует их отчетливую связь с толеитами островных дуг – структур, в которых происходит формирование ювенильных порций континентальной коры.

В статье обобщены литературные данные по 36 объектам находок бонинитов в современных обстановках, офиолитах и раннедокембрийских зеленокаменных поясах. Показано, что породы бонинитовой серии формировались на протяжении всей геологической истории Земли.

Петрологическая уникальность пород бонинитовой серии состоит в том, что для их генезиса требуется сочетание различных факторов, которое может реализовываться только в определенных, и очень ограниченных по месту локализации, геодинамических обстановках. Во-первых, происхождение источника бонинитовых магм требует предварительного истощения верхнемантийного резервуара одним или несколькими эпизодами экстракции базальтовых расплавов; т.е. источником являлась гарцбургитовая мантия. Во-вторых, лавы бонинитовой серии характеризуются заметной обогащенностью крупноионными литофильными элементами и легкими редкоземельными элементами по сравнению с несовместимыми высокозарядными ионами. Такие их геохимические характеристики указывают на активность водного флюида, который должен был быть инфильтрирован в мантийный источник бонинитовых расплавов. Несмотря на неопределенности в экспериментальном моделировании расплавов бонинитовой серии, составы которых зависят от многих факторов, включающих степень деплетации мантии и флюидный режим плавления, существует ясность в том, что для их генерации требуются аномально высокие температуры и присутствие водосодержащего флюида в заметном количестве. На основе современной теории декомпрессионного плавления верхней мантии были проведены расчеты условий генерации первичных расплавов бонинитовой серии различного возраста, что позволило установить отчетливый эволюционный тренд их изменения. Показано, что раннедокембрийские бонинитовые серии формировались при более высоких степенях плавления гарцбургитовой мантии (30–40 %), а формирование мантийных расплавных колонн происходило на существенно бóльших глубинах (3.5–4.0 ГПа), чем в фанерозойском эоне (2.5–3.0 ГПа).

Исследования современных проявлений бонинитового вулканизма демонстрируют, что они локализованы только в зонах интраокеанической плитовой конвергенции, и нет ни одного доказанного примера, свидетельствующего об иных геодинамических обстановках их формирования. Благодаря многочисленным находкам пород бонинитовой серии, в настоящее время стало очевидным, что большинство офиолитов мира маркируют формации не древних срединно-океанических хребтов, а палеозоны спрединга в надсубдукционных обстановках на границах океанических плит геологического прошлого. Понимание геодинамической обстановки формирования бонинитовых серий было связано с тем, что офиолиты супрасубдукционных зон связаны с начальными стадиями возникновения интраокеанических островных дуг. С физической точки зрения, главным условием для начала субдукции является возникновение гравитационной нестабильности в океанической литосфере, приводящей к ее полному расколу или коллапсу, а следовательно, к декомпрессионному плавлению верхней мантии и инициации погружения одной части плиты под другую. Это явление, как и генетическая связь бонинитов с офиолитами, легло в основание «правила инициации субдукции» (subduction initiation rule, SIR) [*Whattam, Stern, 2011*].

Теоретически, коллапс литосферы может произойти в двух случаях: 1) когда в соприкосновение приходят плиты с разными термальными характеристиками, например при трансформном совмещении плит разного возраста – древней, холодной, и молодой, горячей [*Stern, 2004*]; 2) когда место инициации субдукции определяется плотностными неоднородностями на границах нормальной океанической литосферы и утолщенной океанической литосферы плюмовой природы, т.е. океанических плато или трассеров воздействия горячих точек – асейсмических хребтов или симаунтов [*Niu et al., 2003*]. Хорошо известно, что подъем мантийного плюма приводит к ослаблению прочности литосферы и может вызвать раскол континентов. Но, помимо этого явления, внедрение плюма в литосферу существенно изменяет ее плотностные характеристики. Привнос в верхние горизонты мантии и океаническую литосферу расплавов из обогащенного глубинного источника должен приводить к рефертилизации ранее деплетированной мантии. По мере охлаждения такой процесс будет вести к уплотнению переработанной мантийным плюмом верхней мантии, а возникший в области переработки новый сегмент литосферы со временем может приобрести отрицательную плавучесть. Это обусловлено тем, что вулканиты OIB заметно обогащены Fe и Ti. Кроме того, хорошо известно, что Fe-Ti базальты/габбро эклогитизируются гораздо быстрее их магнезиальных эквивалентов.

По-видимому, процесс установления стационарного режима субдукции требует некоторого периода аккомодации, связанного с обрывами слэба и, как следствие, контрастностью тектонических режимов на поверхности. Причиной малоглубинного отрыва слэба могла стать плотностная неоднородность погружавшейся литосферы, например ее локальная переутяжеленность продуктами OIB магматизма. Важнейшими геодинамическими следствиями этого являются, во-первых, кратковременное сильное термальное возмущение над узколокализованной областью слэбового окна и, во-вторых, быстрый аплифт ее надсубдукционной области. Такой механизм хорошо объясняет кратковременность (3–5 млн лет) и большие объемы вулканизма, существенно превышающие объемы вулканизма в режимах стационарной субдукции [*Stern, 2002, 2004*]. Аплифт надсубдукционной области приводит к образованию на месте висячей плиты офиолитовой «платформы» – фундамента для островодужной постройки.

В раннем докембрии бонинитовый магматизм представлен широко, а количество новых находок древних бонинитов неуклонно возрастает. Согласно недавно опубликованным оценкам, объем бонинитового магматизма в архее примерно соответствует объемам коматиитов [*Furnes et al., 2014*]. Установление пород бонинитовой серии, ассоциирующих с фрагментами параллельных даек и метабазитами IAT-типа в древнейшем

сохранившемся комплексе Исуа, по-видимому, указывает на то, что процессы субдукции имеют корни, простирающиеся к началу геологической истории Земли. Поскольку процессы инициации субдукции требуют раскола океанической литосферы на ее полную мощность, раннедокембрийская литосфера по реологическим свойствам до ее основания должна была находиться в области хрупких или хрупко-пластических деформаций. Другими словами, такую литосферу можно рассматривать как жесткое тело, способное противостоять конвективной нестабильности, что является атрибутом плитовой тектоники [*Sleep, 1992*]. Мощность архейской океанической литосферы оценивается в 85–120 км, тогда как современной – примерно в 60 км.

В отличие от фанерозойских бонинитовых серий, родоначальные расплавы раннедокембрийских серий формировались на глубинах ~120–130 км, т.е. в поле стабильности алмаза. Учитывая то, что примитивные расплавы древних бонинитовых серий несут метки субдукционного влияния, можно думать о способности глубокого погружения слэбов в раннедокембрийскую мантию. Таким образом, можно полагать, что в раннем докембрии действовал механизм толстоплитовой тектоники, который к неопротерозою постепенно сменился на механизм тонкоплитовой тектоники. Мантийно-плюмовое воздействие на литосферу Земли – сквозное явление на протяжении всей геологической истории, которое определяет возникновение в ней существенных плотностных неоднородностей и, как следствие, мест инициации субдукции и роста континентальной коры.

Ключевые слова: бониниты; инициация субдукции; мантийный плюм; эволюция геодинамики Земли

The heavy is the root of the light.
(Lao Tzu, *Daodejing*, 5th–4th century BC)

1. Introduction

Boninites attracted much attention at the end of the 20th century, primarily, due to deep-sea studies of forearc slopes in the modern plate convergence zones of the southwestern Pacific. At that time, however, detailed geochemical studies of many ophiolite sections revealed the presence of boninites unknown for mid-oceanic ridges, but abundant in juvenile island-arc basements. Following the common postulation that ophiolites are remnants of the ancient oceanic crust, ophiolites in fold belts were largely interpreted as relic sutures which mark sites of paleo-ocean closure. As the boninite findings were ever-growing in both the classical fragments of the ‘ancient oceanic crust’, e.g. the Troodos in Cyprus, and Semail in Oman, or ‘classical sutures’ such as, the Main Urals Fault in Russia, this inevitably raises the question on the ophiolite nature.

Another problem concerns the evolution of boninitic magmatism as boninites have been discovered in the early Precambrian greenstone belts. Until recently, it was believed that in the early stages of the Earth evolution, ‘dry’ komatiitic volcanism was predominant and then followed by ‘wet’ boninite volcanism [*Hall, Hughes*, *1993*]. However, the komatiite abundance in the Archean seems to be well overestimated. Komatiites are lacking in many belts and constitute less than 5 % of the volcanic rocks in most Archean greenstone belts [*de Wit, Ashwal*, *1997*]. Detailed geochemical studies of mafic-ultramafic complexes in greenstone belts show that a majority of olivine spinifex-free ‘komatiites’ and ‘komatiitic basalts’ belong in fact to the boninite series rocks. According to [*Furnes et al.*, *2014*], boninitic magmatism has been occurred through the geological history of the Earth. However, aspects of its evolution have not been thoroughly discussed in the literature yet.

Thus, the aims of the paper are to provide an overview of the boninitic magmatism occurrences through space and time, track its evolution, and propose a geodynamic explanation of this highly informative phenomenon.

2. Definition and geochemical characteristics of boninites and the boninite series

The International Union of Geological Sciences (IUGS) classification of the high-Mg volcanic rocks defined a boninite as a volcanic rock with the following arbitral chemical composition recalculated to 100 wt %: SiO_2>52 wt %; MgO>8 wt %, and TiO_2<0.5 wt % [*Le Bas*, *2000*]. The Ti content is strongly constrained in the classification as a critical requirement because of titanium is the most incompatible among the major elements, and its low content in primitive melts indicates that their mantle source was highly depleted. Boninite definitions in many publications are very similar to the above-mentioned one. According to [*Crawford et al.*, *1989*], SiO_2 content in boninite lavas exceeds 53 wt %, and Mg#>0.6, where Mg#=Mg/[Mg+Fe^{2+}]. It was recommended in [*Taylor et al.*, *1994*], to classify volcanic and hypabyssal rocks as boninites if SiO_2>53 wt %, TiO_2<0.6 wt %, and 7<MgO<25 wt %.

The above definitions of boninites are based on chemistry, rather than on mineralogy of these rocks. Neither mineralogical nor petrographic characteristics could be included in the classical definition of boninites as the modal mineralogy of phenocrysts show highly variable compositions, and their textural patterns vary widely also. The traditional approach distinguishes between two major groups of boninites, high-Ca and low-Ca [*Crawford et al.*, *1989*], characterized by CaO/Al_2O_3>0.75 and <0.6, respectively. Boninites with intermediate ratios are grouped as low-Ca type 3 boninites. The upper pillow lavas of the Troodos (Cyprus) ophiolite are distinguished as the tectonic and petrographic type of high-Ca boninites. Low-Ca type 1 boninites are best represented by the Cenozoic lavas of New Caledonia. Low-Ca type 2 boninites include high-Mg andesite lavas of the Baja peninsula, California and the Shikoku Island, Japan. The latter of very special geochemical characteristics and tectonic settings have their own names, bajaites and sanukites, respectively [*Rogers, Saunders*, *1989*; *Tatsumi, Ishizaka*, *1981*]. Low-Ca type 3 boninites are most fully represented in the Bonin Islands, Japan where the boninites have been described for the first time at the end of the 19th century.

Despite the fact that two clearly different geochemical groups (high-Ca and low-Ca boninites) are recognized, geodynamic settings for particular types of boninitic magmatism occurrences have not been specified yet [*Meffre et al.*, *1996*]. The assemblage including both high-Ca and low-Ca boninites and intermediate-Ca boninites have been reported from the Mariana island arc [*Arculus et al.*, *1992*]. In other occurrences, such as the Troodos, Oman and Josephine ophiolites, only high-Ca boninites are present [*Cameron*, *1985*; *Crawford et al.*, *1989*; *Ishikawa et al.*, *2002*; *Harper*, *2003*]. Low-Ca and intermediate boninites are dominant in the Ordovician ophiolites of Newfoundland [*Bédard*, *1999*] (Table 1).

Boninites are spatially and genetically related to primitive island-arc low-Ti lavas, thus generating a need for recognition of a separate magmatic series known as 'the boninite series' [*Pearce, Robinson*, *2010; and others*]. The less differentiated rocks of the series are known from the literature as low-Ti tholeiites, LOTI, [*Brown, Jenner*, *1989*] or low-Ti ophiolite basalts [*Sun, Nesbitt*, *1978*], and they are typical of numerous ophiolites. In many cases, the boninite series volcanic rocks are represented mainly by primitive lavas (MgO>12 wt %) that can be termed as picrites or mistakenly classified as komatiitic basalts or basaltic komatiites [*Cameron et al.*, *1979*].

Crystallization of low-Ti tholeiite melts can be schematically given as follows: olivine → clinopyroxene → plagioclase, and the scheme for MORB melts is: olivine → plagioclase → clinopyroxene [*Cameron et al.*, *1980; Natland, 1981*]. This difference is due to drastic distinctions between water-saturated melts of the boninite series and dry melts of the komatiitic and tholeiitic series. The komatiitic series trend is generated by dry mantle melting and directed towards a field of MOR tholeiites, while the boninite series trend reflects the evolution of the primary composition towards the quartz apex, which is typical of wet melting at gradually decreasing temperature and pressure. Distinctions in the compositional trends of the high-Mg volcanic series are well depicted in the projection of the normative basalt tetrahedron Ol-Pl-Qt plotted by using the data on the boninite series of the North Karelian greenstone belt and the komatiitic series of the Kostomuksha greenstone belt in the Baltic Shield (Fig. 1).

The trace elements patterns of the boninites demonstrate strong depletion of the mantle source and concurrent evidences of their suprasubduction genesis, such as, for instance, negative anomalies of Nb(Ta) (Fig. 2). Different types of the boninites have spectra of the same type with distinct negative anomalies of Nb(Ta) and Ti, positive anomalies of Sr and Zr(Hf) and apparent enrichment in large-ionic lithophile (LIL) elements (Rb, Ba, Cs, U, and Th) relative to N-MORB. Such a kind of the trace elements patterns clearly suggests that (i) petrogenesis of boninite series should be excluded any and even a minimum crustal input, and (ii) melting requires a mantle source more depleted in comparison to the mantle lherzolite that generates MORB melts. In other words, melts of the boninite series seem to be derived from a depleted harzburgite mantle source [*Hickey, Frey*, *1982*; *Crawford et al.*, *1989*].

On the other hand, there is geochemical evidence that there is a direct link between the boninite series rocks and island-arc tholeiites (IAT), taking into account the commonly accepted idea that juvenile continental crust portions are generated in the island-arc zones (Fig. 3). Thus, the boninite series rocks are of crucial importance for deciphering crust-forming processes through the geological history of the Earth.

3. Boninites in the geological time and space

The global occurrences of boninite series rocks are shown on Figure 4 and at Table 2. Boninites have been discovered in all the continents, except South America, which is attributable to the fact that South America is still relatively poorly covered by geological studies. The boninite series rocks are described in various sequences through the geologically documented history of the Earth, from the most ancient Eoarchean Isua belt in the southwestern Greenland to the recent eruptions of submarine volcanoes in the northeastern Lau basin. The only lacuna in their history is the Mesoproterozoic, the period of relatively passive tectonic events, possibly

Table 1. **Selected analyses representative of boninite series of different ages which are mentioned in the text and were used for the geochemical plots**

Таблица 1. **Представительные анализы пород бонинитовой серии разного возраста, упоминаемые в тексте и использованные для построения диаграмм**

Location	Northern Tonga		Izu-Bonin-Mariana Forearc			Troodos Ophiolite			Dunzhugur Ophiolite		
Age	2.5–2.7 Ma		48–42 Ma			90–95 Ma			1020 Ma		
Source	*Falloon et al., 2008*		*Pearce et al., 1992*			*Cameron, 1985*			*Sklyarov et al., 2016*		
Type	HCB	HCB	LCB	ICB	HCB	HCB	LOTI	LOTI	LCB	ICB	LOTI
SiO_2 (wt.%)	53.32	55.59	53.47	53.00	47.23	53.80	49.81	51.74	58.09	56.69	48.75
TiO_2	0.24	0.22	0.20	0.25	0.31	0.31	0.19	0.19	0.18	0.18	0.14
Al_2O_3	11.45	14.87	12.05	12.46	12.06	11.40	11.22	12.47	14.41	9.97	16.94
FeO*	9.10	8.25	7.62	6.78	7.24	7.52	8.08	7.20	6.96	7.91	7.45
MnO	0.16	0.13	0.13	0.14	0.14	0.16	0.15	0.15	0.15	0.17	0.14
MgO	13.37	9.19	13.04	13.08	11.40	12.54	13.92	12.74	9.46	13.5	8.9
CaO	8.85	8.92	5.27	6.70	11.90	8.73	10.12	9.88	5.63	6.34	11.04
Na_2O	2.66	1.83	3.19	2.76	2.12	1.30	0.66	1.10	1.46	0.37	2.14
K_2O	0.93	0.80	0.67	0.21	0.26	0.15	0.21	0.39	2.78	3.98	0.78
P_2O_5	0.02	0.03	0.03	0.04	0.04	0.02	0.02	0.01	0.08	0.11	0.02
Mg#	73.4	67.6	76.2	78.4	74.7	76.9	78.4	77.8	71.8	76.2	6.92
Cr (ppm)	812	477	1036	786	762	910	980	940			
Ni	228	124	306	296	374	268	378	339			
Co			45	38.5	44.6						
Sc	44	48	29	33.7	27.1	37	40	40			
V	265	295	166	202	193	212	212	203			
Ba	119	112	47	7.6	15	12	18	45	273	504	127
Rb	5.7	20.3	6.4	3.1	7.6	3	7	7	61.2	68.2	6.8
Sr	118	74	107	136	139	62	53	62			
Nb	1.04	0.96	0.53	0.44	0.53	1	0.8	1	1.16	1.98	0.69
Hf	0.39	0.39	0.9	0.70	0.70	0.7	0.2	0.3	0.82	0.77	0.3
Zr	12.0	12.1	35	27	26	18	10	16	19.9	26.9	10
Y	4.7	4.9	7.2	6.5	8.2	7.3	7	7	7.71	7.7	4.56
Th	0.37	0.37	0.27	0.17	0.18				0.67	0.9	0.3
U	0.19	0.14	0.18	0.12	0.14				0.17	0.44	0.25
La	2.14	1.94	1.81	1.15	1.50	0.88	0.72	1.09	3.59	3.31	1.26
Ce	4.12	3.97	3.86	2.57	3.05	2.22	1.46	2.19	7.77	7.11	2.72
Pr	0.53	0.52	0.59	0.37	0.50	0.36	0.15	0.23	0.76	0.89	0.33
Nd	2.32	2.32	2.84	1.97	2.61	1.91	0.58	1.02	3.41	3.83	1.31
Sm	0.62	0.62	0.81	0.61	0.80	0.73	0.23	0.32	0.94	0.82	0.36
Eu	0.22	0.26	0.27	0.22	0.31	0.27	0.10	0.11	0.24	0.3	0.96
Gd	0.22	0.76	0.97	0.81	1.06	0.96	0.44	0.51	0.94	0.87	0.52
Tb	0.12	0.12	0.16	0.15	0.20	0.20	0.10	0.11	0.17	0.14	0.12
Dy	0.84	0.89	1.05	1.00	1.30	1.39	0.90	0.93	1.06	1.08	0.72
Ho	0.18	0.19	0.23	0.31	0.30	0.32	0.23	0.23	0.22	0.23	0.17
Er	0.56	0.61	0.69	0.72	0.84	1.03	0.76	0.76	0.84	0.66	0.51
Tm	0.09	0.09	0.11	0.12	0.14				0.12	0.12	0.08
Yb	0.61	0.62	0.80	0.75	0.87	1.04	0.84	0.84	0.78	0.77	0.58
Lu	0.10	0.11	0.14	0.11	0.13				0.23	0.13	0.09

Table 1 (end)

Таблица 1 (окончание)

Location	Flin Flon belt		Abitibi greenstone belt			North Karelian greenstone belt			Isua greenstone belt	
Age	1900 Ma		2715 Ma			2800 Ma			3700–3800 Ma	
Source	*Wyman, 1999b*		*Kerrich et al., 1998*			*Shchipansky et al., 2004*			*Polat et al., 2002*	
Type	LCB	HCB	ICB	LOTI	LOTI	LOTI	ICB	HCB	LOTI	LCB
SiO_2 (wt%)	53.8	57.6	59.7	43.8	50.5	49.16	52.80	57.52	49.08	54.00
TiO_2	0.12	0.09	0.31	0.18	0.24	0.42	0.47	0.35	0.23	0.40
Al_2O_3	14.50	7.6	15.8	15.8	14.1	10.65	13.03	9.39	16.94	17.74
FeO*	9.81	9.27	6.90	10.1	9.70	11.03	10.90	9.53	9.12	8.37
MnO	0.10	0.2	0.50	0.21	0.27	0.19	0.17	0.17	0.17	0.13
MgO	11.1	12.6	7.37	22.0	15.0	12.92	10.35	12.80	15.57	7.05
CaO	5.0	9.6	6.59	6.7	6.18	11.37	7.37	6.86	6.82	8.39
Na_2O	3.7	0.6	1.98	0.12	2.48	0.35	2.44	0.07	0.95	2.85
K_2O	0.8	1.5	0.01	0.01	0.01	0.07	0.08	0.10	0.09	0.12
P_2O_5	0.01	0.02	0.06	0.03	0.03	0.13	0.10	0.08	0.01	0.02
Mg#	68.0	71.9	69.0	80.0	74.0	0.71	66.0	71.8	77.0	63.0
Cr (ppm)	544	1411	330	1460	1058	706	324	540	951	141
Ni	155	183	210	760	499	254	187	189	376	69
Co	65	59	51	74	71.3	74	53	51	63	35
Sc	85	49	55	48	44	38	40	33	42	45
V	319	170	250	250	160	238	339	202	192	195
Ba						15.8	18	12	8	14
Rb						0.92	1.2	2.7	7.1	4.3
Sr						49	63	69.5	54	116
Nb	1.2	0.6	1.3	0.42	0.71	0.88	1.01	1.06	0.15	0.55
Hf	0.71	0.35	0.64	0.3	0.38	0.89	0.83	0.75		1.1
Zr	26	14	26	12	16	34	29	26.5	16.4	27.5
Y	5.0	3.0	17	9	10	12.2	13.9	0.17	9.2	13
Th	0.36	0.2	0.2	0.05	0.09	0.09	0.13	0.08	0.08	0.23
U	0.31	0.16			0.01	0.04	0.04	0.02		
La	1.78	1.21	1.46	0.49	0.72	0.78	1.16	1.39	0.46	1.26
Ce	4.11	2.67	3.87	1.33	1.81	2.51	3.49	3.55	1.26	3.08
Pr	0.51	0.31	0.59	0.21	0.27	0.39	0.55	0.52	0.20	0.46
Nd	2.18	1.32	2.62	1.11	1.33	2.05	3.42	2.57	1.10	2.28
Sm	0.58	0.33	0.74	0.39	0.45	0.73	0.99	0.82	0.44	0.91
Eu	0.23	0.12	0.19	0.14	0.24	0.35	0.39	0.29	0.13	0.28
Gd	0.76	0.45	1.19	0.63	0.67	1.31	1.62	1.37	0.69	1.32
Tb	0.13	0.07	0.26	0.14	0.14	0.24	0.27	0.27	0.16	0.26
Dy	0.89	0.43	2.54	1.32	1.22	1.77	2.03	1.78	1.33	2.04
Ho	0.19	0.1	0.65	0.36	0.31	0.41	0.45	0.43	0.37	0.54
Er	0.55	0.29	2.33	1.23	0.95	1.20	1.32	1.26	1.36	1.91
Tm	0.10	0.05	0.39	0.22	0.17	0.17	0.18	0.19	0.21	0.28
Yb	0.55	0.3	3.03	1.49	1.19	1.05	1.24	1.18	1.49	1.83
Lu	0.10	0.05	0.50	0.24	0.18	0.15	0.19	0.19	0.24	0.28

N o t e. HCB – High-Ca boninite, ICB – intermediate-Ca boninite, LCB – Low-Ca boninite; LOTI – Low-Ti basalt/picrite. Subdivision of boninites is after [*Crawford et al., 1989*].

П р и м е ч а н и е. HCB – высококальциевые бониниты, ICB – умереннокальциевые бониниты, LCB – низкокальциевые бониниты, LOTI – низкотитанистые базальты/пикриты. Разделение бонинитов по [*Crawford et al., 1989*].

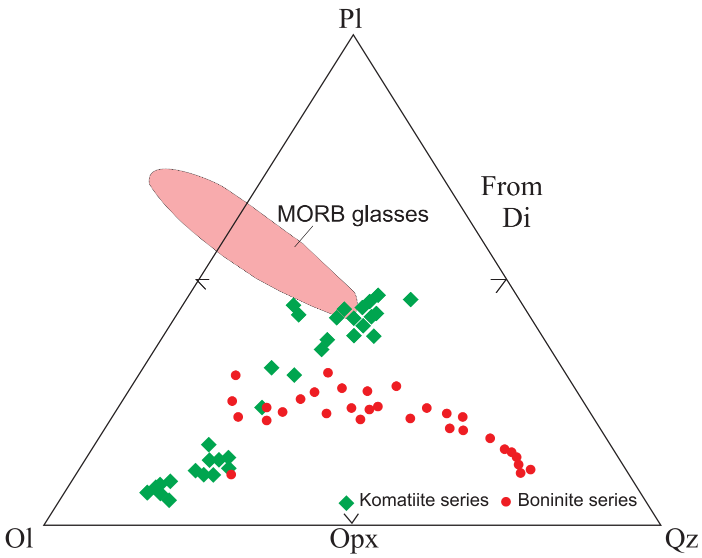

Fig. 1. A comparison between normative compositional trends of the boninite and komatiite volcanic series in ternary projection olivine-plagioclase-quartz from diopside [*Walker et al., 1979*]. The both volcanic series are from the Archean Karelian Craton. Modified after [*Shchipansky, 2008*].

Рис. 1. Положение фигуративных точек состава позднеархейских высокомагнезиальных вулканитов Карельской ГЗО в проекции нормативного базальтового тетраэдра Ol-Pl-Qz из вершины диопсида (Di) [*Walker et al., 1979*]. Обе вулканические серии из архейского Карельского кратона. Модифицировано из работы [*Shchipansky, 2008*].

related to the existence of the stable supercontinent Nuna [*Cawood, Hawkesworth, 2014*].

Contemporary settings for generation of the boninite series rocks are known in the areas of intraoceanic island-arc systems of the southwestern Pacific, specifically the Izu-Bonini-Mariana (IBM) and Tonga-Kermadec island arcs. Boninites compose mostly fore-arc slopes, forming the lowest stratigraphic levels in the island-arc architecture. These regions are natural laboratories for comprehensive studies of the boninitic magmatism coupled with geodynamic modeling of its genesis. It is noteworthy that since the Paleocene onwards there is a strong link between boninites and ophiolites, as confirmed by the data on the Cape Vogel Peninsula, Papua New Guinea (see Table 2). Actually, this genetic link has long been known [*Sun, Nesbitt, 1978*; *Cameron et al., 1979*] and led to introduction of the term 'suprasubduction zone (SSZ) ophiolite' in the 1980s to acknowledge that some ophiolites are more closely related to island arcs than to ocean ridges [*Pearce, 1982*]. This term was readily accepted in the literature, and the majority of the known ophiolite complexes, including the largest ones with the completely preserved sequences, e.g. Troodos, Oman, were classified into the SSZ type.

According to [*Sklyarov et al., 2016*], there are four main types of boninites in the ophiolite sequences (Fig. 5). Type 1 bonninites spatially coexists with ophiolites, although compose (or belong to) other tectonic units. Type 2 boninites presents as later constituents of ophiolite sequences, such as crosscutting dikes or lavas on top of section. Type 3 includes island-arc tholeiites and basaltic andesites coupled with boninites, which are replaced by younger MORB or BABB affinities. Type 4 boninites occupies the whole mafic portion of ophiolite sequences, together with island-arc tholeiites and basaltic andesites, and all the components of such sequences (gabbro, dykes, and lavas) have clearly boninitic affinities.

These types of the boninite-bearing ophiolite sequences are recorded through the entire Phanerozoic and Neoproterozoic. The Neoproterozoic boninite

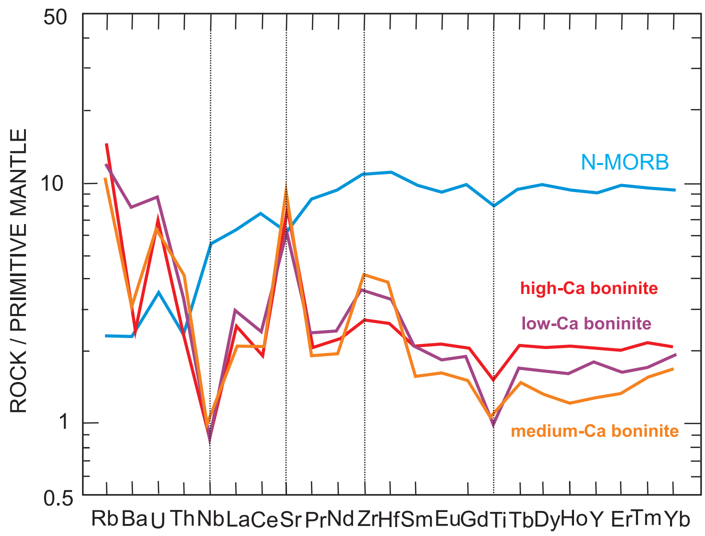

Fig. 2. Trace elements patterns of different boninite groups from Izu-Bonin arc by comparison with N-MORB.

Note the negative anomalies of Nb (Ta) and, conversely, positive anomalies of Zr (Hf) and Sr, both typical of supra-subduction zone volcanics. Strong depletion in REE and HFSE of the boninite compositions with respect to N-MORB is clearly visible. Averaged boninite compositions are from [*Pearce et al., 1992*]. N-MORB and primitive mantle values are from [*Hofmann, 1988*].

Рис. 2. Мультиэлементные диаграммы разных геохимических групп бонинитов Изу-Бонинской островной дуги.

Заметим характерные для бонинитов и индикаторные для петрогенезиса вулканитов в надсубдукционных обстановках отрицательные аномалии Nb (Ta) и Ti и, наоборот, положительные Zr (Hf) и Sr. Ясно видны также геохимические различия в уровне общей деплетации некогерентными элементами между бонинитами и толеитами MORB. Составы бонинитов по [*Pearce et al., 1992*]. Примитивная мантия и MORB по [*Hofmann, 1988*].

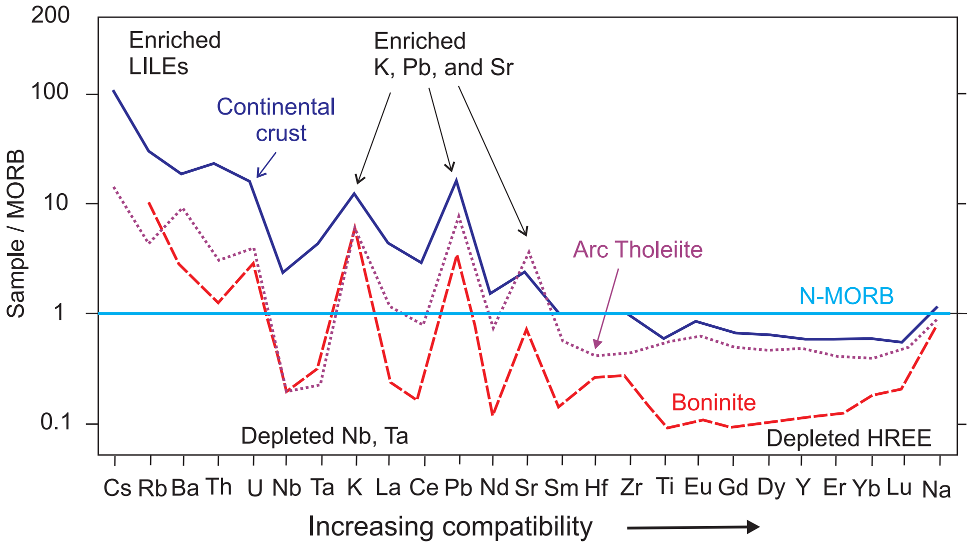

Fig. 3. Spidergram for trace-element compositions of the continental crust and juvenile arc melts (boninite, arc tholeiite), modified after [*Stern, 2002*].

Elements on the horizontal axis are listed in order of their incompatibility in the mantle relative to melt; elements on the left are strongly partitioned into the melt whereas those on the right are strongly partitioned into a peridotite source. Note the characteristic enrichments of subduction zone outputs relative to MORB with respect to fluid-mobile LIL elements and the relative depletion of these in HFSE, and HREE. Note also the overall similarity of continental crust to juvenile arc crust.

Рис. 3. Спайдерограмма распределения малых элементов в континентальной коре и в расплавах ювенильных островных дуг (бонинита и островодужного толеита), модифицировано из работы [*Stern, 2002*].

По горизонтальной оси графика элементы расположены в порядке их несовместимости в мантии относительно расплавной фазы. В левой части спектров расположены элементы, совместимые с расплавами; в правой части – совместимые с перидотитовым источником. Заметим характерное для субдукционных зон обогащение мобильными крупноионными элементами, связанное с флюидным привносом, и, наоборот, деплетацию высокозарядных ионов и тяжелых редких земель по сравнению с N-MORB. Обращает на себя внимание общее сходство геохимии континентальной коры и ювенильной коры островных дуг.

series are widely distributed in the Altai-Sayan area of the southern frame of the Siberian Craton [*Simonov et al., 1994*; *Dobretsov et al., 2005*]. More ancient boninite series are discovered in the Archean and Paleoproterozoic metamorphosed fold belts that are often jointly termed as ‘greenstone belts’, regardless of the metamorphic grade.

As a rule, the rock assemblages composing the greenstone belts were strongly tectonically transformed and dismembered that gives a zero chance for preservation of a complete ophiolite sequence. Nonetheless, the Early Precambrian greenstone belts maintain vestiges indicating that rock assemblages of oceanic provenance were involved in the tectogenesis of the belts [*Shchipansky*, *2008*; *Rosen et al.*, *2008*; *Furnes et al.*, *2015*]. These are mainly the isotopic and geochemical signatures of the lack of crustal contamination or affiliation of the mafic-ultramafic assemblages of the greenstone belts to the ensimatic island-arc settings. In the latter case, the presence of the boninite series rocks is a critical support to the suprasubduction ophiolite interpretation of the greenstone belts sequences.

Besides the isotope-geochemical data, some boninite series from the Archean greenstone belts do preserve field evidences on the ocean lithosphere extension. We reported a fragment of the suprasubduction ophiolites with sheeted dikes in gabbroids and metalavas of the boninite series (~2.8 billion years) in the Iringora locality of the North-Karelian greenstone belt [*Shchipansky et al.*, *2001*, *2004*]. Later on, relics of a sheeted-dike complex were discovered in the Garbenchifer formation from the Eoarchean Isua supracrustal belt, southwestern Greenland [*Furnes et al.*, *2007*, *2009*]. This suggests that the boninite series rocks and the SSZ spreading have been genetically related since the early stages of the Earth's geological history.

The early Precambrian boninite series differ from the Phanerozoic ones by the presence of both boninites and komatiites in some greenstone belts, such as the Bogoin (Paleoproterozoic), Abitibi (Neoarchean), and Koolyanobbing (Mesoarchean) belts, which is related to mantle plume fingerprinting into intra-oceanic convergence zones (see Table 2). It should be noted, however, that data on the Phanerozoic boninite series often

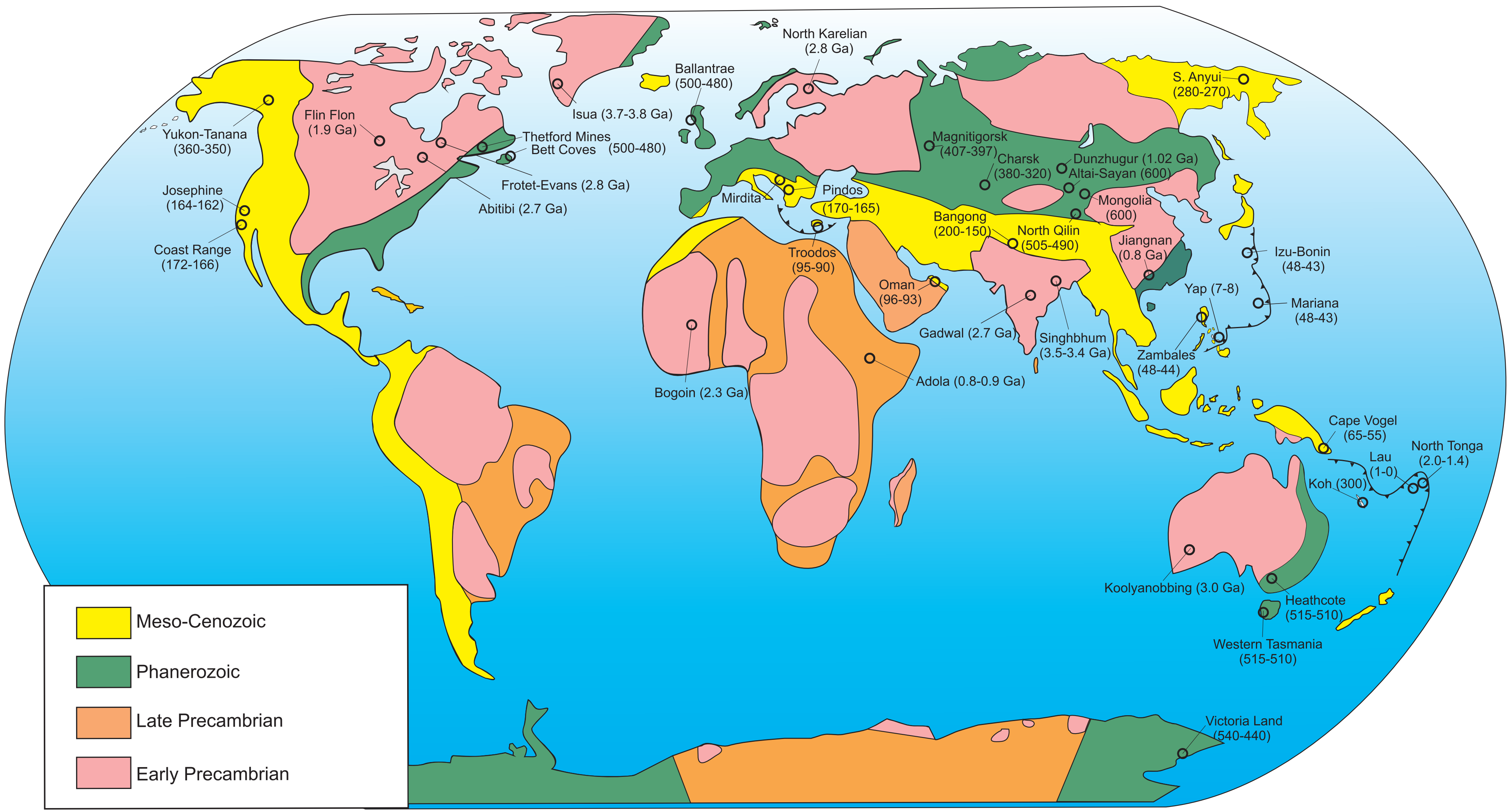

Fig. 4. Global map of boninite occurrences from which boninite series rocks have been reported and described in details. See Table 1 for references.

Рис. 4. Распространение бонинитов на земном шаре, детальное описание находок которых было приведено в литературе. См. таблицу 1, где приведены соответствующие ссылки.

Т a b l e 2. **Global occurrences of boninite series volcanics with some short comments on their tectonic characteristics**

Т а б л и ц а 2. **Распространенность вулканитов бонинитовой серии на земном шаре и краткая характеристика областей их локализации**

Locality	Age	Tectonic setting	Geodynamic implication	References
NE Lau Basin	Modern submarine explosions	Multi-spreading centre	Nascent juvenile island arc above a subduction zone	*Resing et al., 2011*
Northern termination of the Tonga trench	2.5–2.7 Ma	Fore-arc slope	Supra-subduction extensional zone in an island arc basement	*Falloon et al., 2008; Sobolev, Danyushevsky, 1994; Falloon, Crawford, 1991*
Yap trench, Philippine sea	7–8 Ma	Trench slope	Supra-subduction extensional zone in a forearc setting	*Crawford et al., 1986*
Izu-Bonin-Mariana Island Arc	48–42 Ma	Fore-arc slope	Nascent juvenile island arc above a subduction zone	*Crawford et al., 1981; Crawford et al., 1989; Stern et al., 1991; Stern, Bloomer, 1992; Stern, 2004; Taylor et al., 1994; Li et al., 2013*
Luzon, Philippines	48–44 Ma	Complete SSZ ophiolite sequence	Basement of an juvenal island arc	*Yumul, 1996; Yumul et al., 2000*
Cape Vogel Peninsula, PNG	Paleocene	Papuan Ultramafic Belt	Supra-subduction extensional zone in a forearc setting	*Walker, Cameron, 1983; Crawford et al., 1989*
Troodos Massif, Cyprus	90–95 Ma	Complete SSZ ophiolite sequence	Nascent juvenile island arc above a zone of subduction initiation	*Sun, Nesbitt, 1978; Cameron et al., 1980; Cameron, 1985; Sobolev et al., 1993; Pearce, Robinson, 2010; Whattam, Stern, 2011*
Pindos Ophiolite Complex, NW Greece	170–165 Ma	Complete SSZ ophiolite sequence	Supra-subduction extensional zone in a forearc setting	*Pe-Piper et al., 2004*
Mirdita Ophiolite Complex, northern Albania	Jurassic	Complete SSZ ophiolite sequence	Supra-subduction extensional zone in a forearc setting possibly related to the MOR subduction	*Bortolloti et al., 1996; Bortolloti et al., 2002*
Josephine Ohiolite, Klamath Mountains, NW California	164–162 Ma	Complete SSZ ophiolite sequence	Progradation of a spreading centre from backarc basin to the forearc area of the juvenile island arc	*Harper, 1984; Harper, 2003; Wallin, Metcalf, 1998; Metcalf, Shervais, 2008*
Coast Range ophiolites, California	172–166 Ma	Ophiolite remnants in serpentinite matrix mélange	Supra-subduction extensional zone in a forearc setting possibly related to the MOR centers subduction	*Shervais, 2001; Shervais et al., 2004 Shervais et al., 2005*
Bangong Lake ophiolite, NW Tibet	Early Jurassic	Ophiolite remnants in serpentinite matrix mélange	Supra-subduction extensional zone in a forearc setting	*Shi et al., 2004; Shi et al., 2008*
South Anyui suture ophiolite, Western Chukotka	280–270 Ma	Gabbro, gabbro-pyroxenite, and restitic ultra-mfic rocks of an ophiolite sequence	Supra-subduction extensional zone in a forearc or backarc settings	*Ganelin, Silantjev, 2008*

Т а b l e 2 (continued)

Т а б л и ц а 2 (продолжение)

Locality	Age	Tectonic setting	Geodynamic implication	References
Koh Ophiolite, New Caledonia	295 Ma	Upper lavas of the complete SSZ ophiolite	Progradation of a spreading centre from backarc basin to the forearc area of the juvenile island arc	*Meffre et al., 1996; Aitchison et al., 1998*
Charsk belt, Eastern Kazakhstan	Late Devonian – Early Carboniferous	Mafic to acid volcanics associated with dismembered ophiolites	Supra-subduction environment	*Simonov et al., 2010*
Yukon-Tanana terrane, SW Yukon, Canada	Pre Late Devonian	Fire Lake boninitic rocks containing volcanic-hosted massive sulfide deposits	Progradation of spreading ridge into a suprasubduction environment	*Piercey et al., 2001*
Magnitogorsk juvenile island arc of the Sakmar zone in the South Ural	Early Devonian	Volcanics and dykes from the SSZ ophiolite sequences	Supra-subduction extensional zone in a basement of juvenal arc	*Spadea et al., 1998; Kosarev et al., 2005; Puchkov, 2010; Belova et al., 2010*
Ballantrae complex ophiolite, Southwest Scotland	500–480 Ma	Volcanics from the SSZ ophiolite sequences	Fragment of an intra-oceanic island arc	*Smellie et al., 1995*
Thetford Mines Ohiolite, Canadian Appalachians	500–480 Ma	Volcanics from the SSZ ophiolite sequences	Supra-subduction extensional zone in a forearc setting	*Page et al., 2009*
Betts Cove ophiolite, Newfoundland, Canada	500–480 Ma	Volcanics from the SSZ ophiolite sequences	Supra-subduction extensional zone in a forearc setting	*Bédard et al., 1998; Bédard, 1999*
Ophiolite of Western Tasmania	Early Cambrian	Lavas associated with ophiolitic ultramafic complexes	Supra-subduction extensional zone in a forearc setting	*Brown, Jenner, 1989; Crawford, Berry, 1992*
Heathcote Greenstone belt in the Lachlan Fold Belt, SE Australia	Early Cambrian	The oldest metavolcanics in the Lachlan Foldbelt	Supra-subduction extensional zone in an island arc setting	*Crawford, Cameron, 1985*
Tholeiite-boninitic terraine of the North Qilian suture zone, China	Early Cambrian	The volcanic complex of the North Qilian ophiolite belt	Nascent juvenile island arc above a subduction zone.	*Xia et al., 2012*
Boninite-derived amphibolites from the Lanterman-Mariner suture, Victoria Land	Cambrian – Ordovic	Boninite-derived retrogressed amphibolites within the Early Paleozoic sure zone	Juvenile island arc or backarc basin	*Palmeri et al., 2012*
Boninite series of the Altai-Sayan Fold Belt	Vendian-Cambrian	Lavas, dykes and gabbro of boninitic affinity from dismembered or partially preserved SSZ ophiolite sequences	Subduction initiation of the nascent juvenile island arcs	*Simonov et al., 1994; Dobretsov et al., 2005*
Boninite-series rocks from the ophiolites of Western Mongolia	Vendian-Cambrian (~600 Ma)	Lavas, dykes and gabbro of boninitic affinity from the Khantaishir and Bayannor Ranges Ophiolites	Forearc or backarc extensional basins	*Zonenshain, Kuzmin, 1978; Kepezhiskas et al., 1991; Khain et al., 2003*
Boninite-series rocks from the Jiangnan Fold Belt, SW Cina	850–825 Ma	Greenschist-facies boninite series rocks of the SSZ opniolite conplex from the Xiuning–Shexian Fault zone	Nascent juvenile island arc above a subduction zone	*Zhao, Asimov, 2014*

Table 2 (end)

Таблица 2 (окончание)

Locality	Age	Tectonic setting	Geodynamic implication	References
Adola boninite from the Megado ophiolitic belt, Southern Ethiopia	790 Ma	Low-grade boninite series rocks of the Megado SSZ ophiolite	Supra-subduction extensional zone in a forearc or backarc settings	*Wolde et al., 1996; Yibas et al., 2003*
Dunzhugur boninite series of the Ilchir Ohiolite Belt, Eastern Sayan, Russia	1020 Ma	Lavas, dykes and gabbro of boninitic affinity from the upper part of ophiolite sequence	Nascent juvenile island arc above a subduction zone	*Dobretsov et al., 1986; Khain et al., 2002; Kuzmichev, 2004*
Boninites of the Flin Flon greenstone belt, Trans-Hudzon Orogen, Canada	1900 Ma	Low grade subaqueous lavas in the lowermost part of the island arc volcanics	Supra-subduction extensional zone in a forearc or backarc settings	*Stern et al., 1995; Leybourne et al., 1997; Wyman, 1999a*
Bogoin boninite-like rocks of the Bogoin-Boali greenstone belt, Central African Republic	2300 Ma	Upper pillowed amphibolites underlined by Al-depleted and Al-undepleted komatiites and meta-greywackes	Accretionary complex in a convergent plate margin	*Poidevin, 1994*
Boninites from the Gadwal grrenstone belt, Eastern Dharwar Craton, India	2700–2500 Ma	Amphibolite-facies boninite series occurred along with pillowed metatholeiites	Subduction environments of small plate tectonics involving an interaction of mantle plume and inta-oceanic island arc	*Manikyamba et al., 2005; Manikyamba, Kerrich, 2012*
Boninite series of the Abitibi greenstone belt	2715 Ma	Greenschist-facies volcanics Wihtney underlined by Al-depleted and Al-undepleted komatiites Kidd-Munro	Accretionary complex emerged by interaction of mantle plume and inta-oceanic island arc	*Kerrich et al., 1988; Wyman, 1999a; Wyman, 1999b*
Boninite series volcanics of the Frotet-Evans greenstone belt, Opatica, Superior, Canada	2790 Ma	Low-grade boninitic ricks of the lowermost part of the arc-related Assinica group sequence	Supra-subduction extensional zone in a forearc setting	*Boily, Dion, 2002*
Boninite series of the North Karelian greenstone belt, Baltic Shield, Russia	2804 Ma	Amphibolite-facies boninite-series rocks from the upper part of the SSZ ophiolite complex	Nascent juvenile island arc above a subduction zone	*Shchipansky et al., 1999; Shchipansky et al., 2001; Bibikova et al., 2003; Shchipansky et al., 2004 Shchipansky, 2008*
Boninite series of the Koolyanobbing greenstone belt, Craton Yilgarn, SW Australia	3023 Ma	Amphibolite-facies boninite-series rocks alternated with komattite-tholeiite series volcanics in the lower part of the Koolyanobbing sequence	Accretionary complex emerged by interaction of mantle plume and intra-oceanic island arc	*Angerer et al., 2013*
Boninite series of the Older Metamorphic Group of the Singhbhum Craton, eastern India	3550–3440 Ma	Amphibolite-facies boninite-series rocks associated with metapelites and BIFs	One of the first evidences on a subduction initiation at the Archean	*Manikyamba et al., 2015*
Boninite-series of the Isua greenstone belt, SW Greenland)	3800 Ma	Amphibolite-facies boninite-series rocks of Garbenchifer Formation associated with IAT and BIFs.	First evidence on a subduction initiation and oceanic lithosphere extension in the Earth history	*Polat et al., 2002; Polat, Hoffman, 2003; Furnes et al., 2007; Furnes et al., 2009*

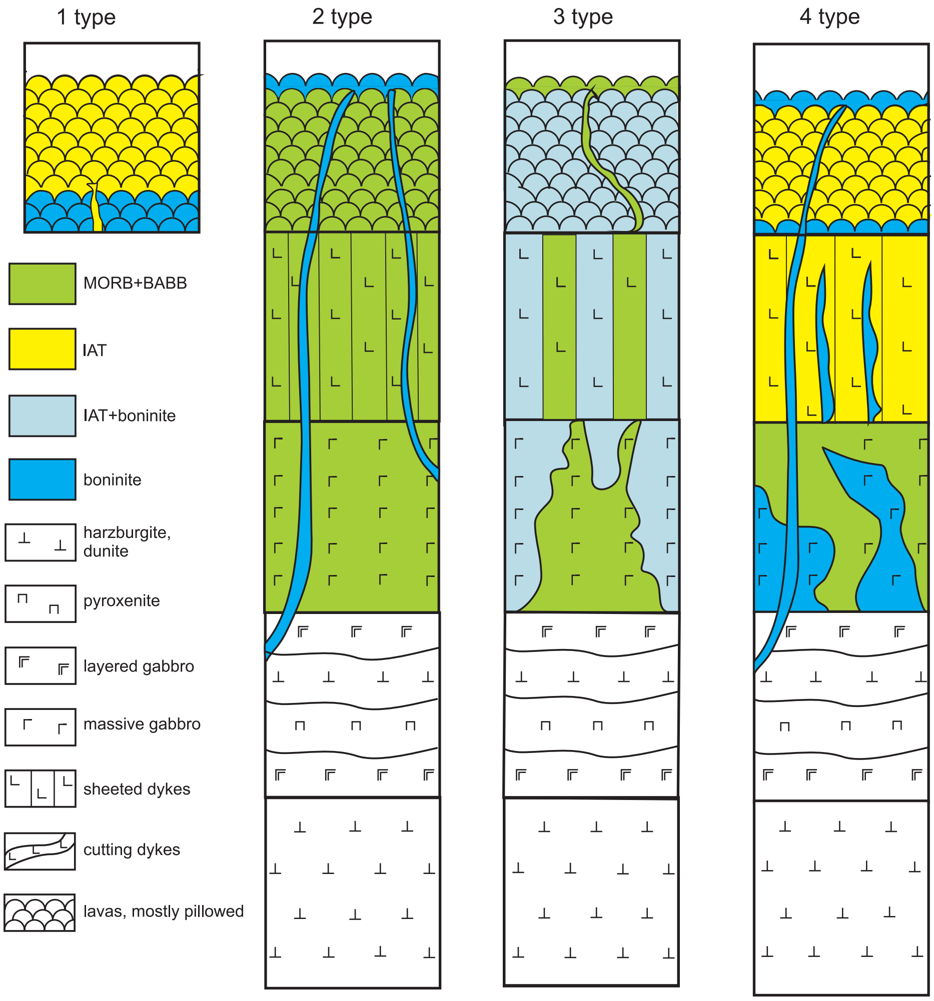

Fig. 5. Models illustrating four tectonic types of boninite occurrences in ophiolitic sections, after [*Sklyarov et al., 2016*].

Рис. 5. Идеализированные разрезы «тектонических» типов бонинитов, по [*Sklyarov et al., 2016*].

suggest the mantle plume involvement in their petrogenesis that will be discussed below.

4. Petrogenesis of the boninite series rocks, and their evolution in time

The boninite series rocks are unique because of their genesis requires the set of conditions which is possible only in specific geodynamic settings within spatially limited locations. Indeed, the origin of a boninite source requires prior depletion of an upper mantle reservoir by basalt melt extraction in one or several episodes, which means that mantle harzburgite was such a source [*Hickey, Frey, 1982*; *Sun, Nesbitt, 1978*; *Duncan, Green, 1980, 1987*]. Boninitic melts are primitive and, at the same time, highly silicic with very low absolute concentrations of incompatible trace elements (Nb, Ta, and Ti) and rare earth elements; this suggests melting of residue peridotite at relatively shallow depths.

In fact, contents of Cr and Ni in the boninite series rocks are high. The strong and fast depletion in Cr suggests that chromite was among the main liquidus phases at the early stages of the primary melt fractionation. Depletion in Ni and simultaneously increasing contents of SiO_2 indicate that olivine played an important role in magmas fractionation to Mg#~0.70. As noted above, the subsequent crystallization phase was clinopyroxene replaced then by plagioclase.

The boninite series lavas are considerably enriched in LILE and LREE in comparison to HFSE. Such geochemical characteristics suggest active infiltration of hydrous fluid into the mantle source of the boninite melts [*Pearce et al., 1984, 1992*; *Pearce, 1982, 2003*; *Crawford et al., 1989*; *Bloomer et al., 1995*; *Stern et al., 1991*]. The presence of fluid water in the mantle wedge is also a prerequisite to lower the solidus melting temperature of a refractory source.

While the ideas concerning the source of the boninite series melts are commonly consistent, there is a disagreement in estimated P–T conditions for generation of parental magmas, i.e. primitive high-Mg and low-silica melts [*Cameron*, *1985*]. In [*Duncan, Green*, *1980*, *1987*], the MgO content is estimated at 15–16 % for the primary Troodos boninite series melts generated by mantle harzburgite melting at 7–8 kbar at a temperature of 1360 °C. In [*Sobolev et al.*, *1993*], P-T estimates show larger depths and higher temperatures: 2–3 GPa; 1380–1450 °C; MgO content of 17–22 wt %. Resulting from the melt inclusion studies, the Neoproterozoic boninite series from the Altai-Sayan segment of the Central-Asian fold belt were crystallized at T~1330–1150 °C from a water-saturated (up to 3.9 wt % H_2O) primary melt at depths of about from 60 to 90 km [*Dobretsov et al.*, *2005*].

It has been experimentally determined [*Kushiro*, *1990*] that adding 4.4–6.6 wt % H_2O into the mantle substance reduces the melting start pressure by almost 2 kbar and lowers the temperature by ~150 °C. Experiments with refractory harzburgite under anhydrous and H_2O-undersaturated conditions [*Falloon, Danyushevsky*, *2000*] show that the high-Ca boninite petrogenesis requires temperatures as high as ~1480 °C and a pressure of about 1.5–2 GPa in the presence of 2–3 wt % H_2O.

Notwithstanding significant uncertainties in the boninite series melt models (which compositions are dependent on many factors, including the mantle depletion degree and the fluid melting mode), there is a general consensus that their genesis requires anomalously high temperatures and the presence of a water-containing fluid in considerable quantities. In this case, temperature anomalies mean temperature values considerably exceeding those in the ambient upper mantle, which are sufficient for MORB generation. In the recently introduced theory on decompression melting of the upper mantle, a potential mantle temperature (*Tp*), i.e. a temperature at the lowest point of the mantle column, is set at ~1350 °C for generation of the parental melt for N-MORB [*Langmuir et al.*, *1992*; *O'Hara, Herzberg*, *2002*]. This melt corresponds to a picrite composition (13 wt % MgO), and MORB13 composition model is perfectly matched to the fractionation trend of tholeiitic melts forming N-MORB [*Niu, O'Hara*, *2009*]. Figure 6 illustrates the idea that the generation conditions of the boninite series rocks and MORB are different. Comparison of the MORB and boninite compositions with similar Mg –number gives grounds to challenge the geodynamic model suggesting that boninites could form in zones of stretching above the mid-ocean ridges in supra-subduction environments (see also [*Metcalf, Shervais*, *2008*]). What petrogenetic conditions may be responsible for the boninite series rock genesis? Did any evolutionary changes occur in such conditions through the Earth's history?

Answers to the above questions can be derived from the theory of upper mantle decompression melting and its key concept of accumulated fractional melting. If the latter is the case, the mantle source begins to melt in small amounts during decompression; typically, melt is extracted after 1–2 % melting by buoyancy-driven porous flow; and the residue continues to melt in small increments during decompression. This process takes place repeatedly as decompression progresses from an initial high to a final low melting pressure. The small melt fractions mix in transitional crustal magma chambers to make an aggregate primary magma melt. Each melt droplet contributing to the aggregate is in equilibrium with a specific source which composition varies from the initial relatively fertile to the depleted final composition. An aggregate fractional melt is not in equilibrium with its residue; only the final drop of the melt extracted is in equilibrium with the residue [*Herzberg, Rudnick*, *2012*]. In solutions of the mass balance equation, mean values of residue, pressure and melt amount are used for simplicity. This facilitates solving

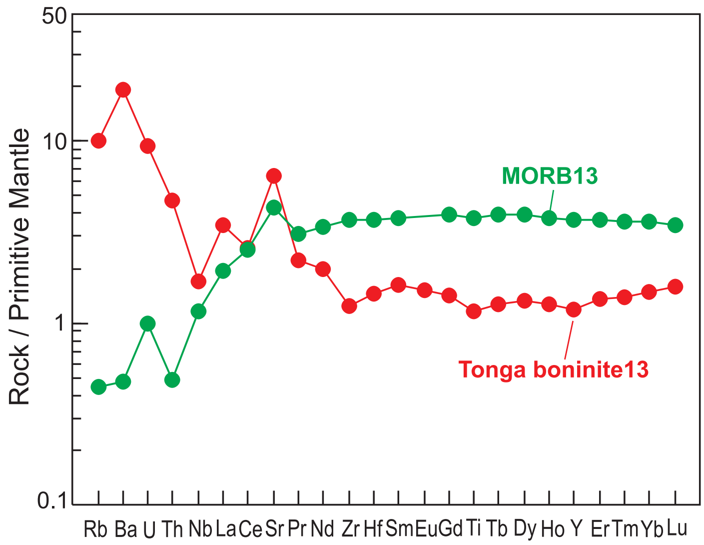

Fig. 6. A comparison between trace element compositions of the parental melt for modern MORB expressed as MORB13 [*Niu, O'Hara, 2009*] and the recent boninite with ~13 wt. % MgO from the Tonga fore-arc [*Falloon et al., 2008*].

It is clear that a petrogenesis of boninite series seems to be unrelated with an extensional environment characteristic of a MORB-forming magmatic column. Primitive mantle values are from [*Hofmann, 1988*].

Рис. 6. Сравнение состава малых элементов родоначального расплава современных MORB, выраженного как MORB13 [*Niu, O'Hara, 2009*], и современного бонинита с содержанием MgO ~13 вес. % из преддуговой области Тонга [*Falloon et al., 2008*].

Из рисунка следует, что петрогенезис бонинитовой серии не может быть связан с обстановками растяжения, в которых образуются расплавные колонны толеитов MORB-типа. Примитивная мантия по [*Hofmann, 1988*].

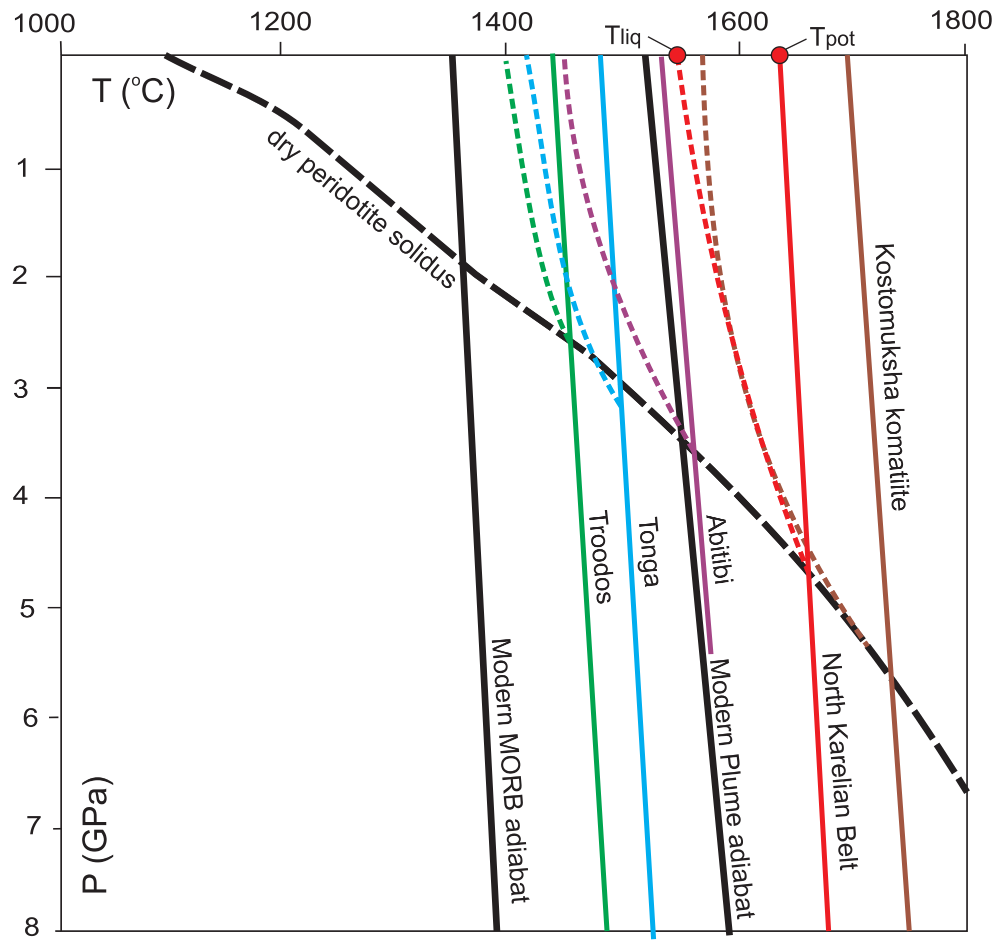

Fig. 7. A plot illustrating possible relationships between mantle potential temperatures (T_P) and primitive magma liquidus temperatures (T_{liq}) for the modern boninite series (Tonga, Troodos) and the Archean ones (Abitibi, North Karelian greenstone belt).

The diagram is simplified by showing a dry solidus applicable to both MORB and the boninite series, because a hydrous melting will take place below the dry solidus and the boninite series have a more depleted mantle solidus than MORBs. T_p and T_{liq} for boninite series rocks have been calculated from the appropriated compositions using software PRIMELT2.XLS [*Herzberg, Asimow, 2008*]. Data source: Troodos [*Pearce, Robinson, 2010*]; Tonga [*Falloon et al., 2008*]; Abitibi [*Kerrich et al., 1998*]; North Karelian greenstone belt [*Shchipansky et al., 2004*]. Data for the Kostomuksha komatiites were taken from [*Puchtel et al., 1998*].

Рис. 7. Иллюстрация соотношений между мантийными потенциальными температурами (Tp) и ликвидусными температурами (T_{liq}) примитивных магм современных (Тонга, Троодос) и архейских (Абитиби, Северо-Карельский зеленокаменный пояс) бонинитовых серий.

Диаграмма показывает упрощенные соотношения, поскольку показаны солидусы безводного плавления; в природе мокрое плавление будет понижать солидус, а источник для бонинитовых серий является более деплетированным и тугоплавким, чем источник для MORB. T_p и T_{liq} рассчитаны по выборке соответствующих условиям моделирования составов с помощью программы PRIMELT2.XLS [*Herzberg, Asimow, 2008*]. Источники данных: Троодос [*Pearce, Robinson, 2010*], Тонга [*Falloon et al., 2008*], Абитиби [*Kerrich et al., 1998*], Северо-Карельский пояс [*Shchipansky et al., 2004*]. Для сравнения показаны данные по коматиитам Костомукши по [*Puchtel et al., 1998*].

general problems of decompression melting with regard to the mantle columns formed in differing, i.e. plume or mid-ocean ridge, settings. Using the data on the most primitive compositions, that are mainly controlled by olivine fractionation, it becomes possible to calculate parental melt compositions and potential mantle temperatures corresponding to the melting initiation depth of the given mantle column [*Herzberg et al., 2007*; *Herzberg, Asimow, 2008*].

Figure 7 illustrates relationships between potential and liquidus temperatures of the most primitive compositions of the modern (Tonga forearc and Troodos and upper pillow lavas) and Archean (Abitibi and North Karelian greenstone belts) boninite series. The potential mantle temperatures for their generation differ by 150–200 °C. This difference refers to the assemblages generated by mantle sources of an almost similar type (mantle harzburgite) due to its melting in the

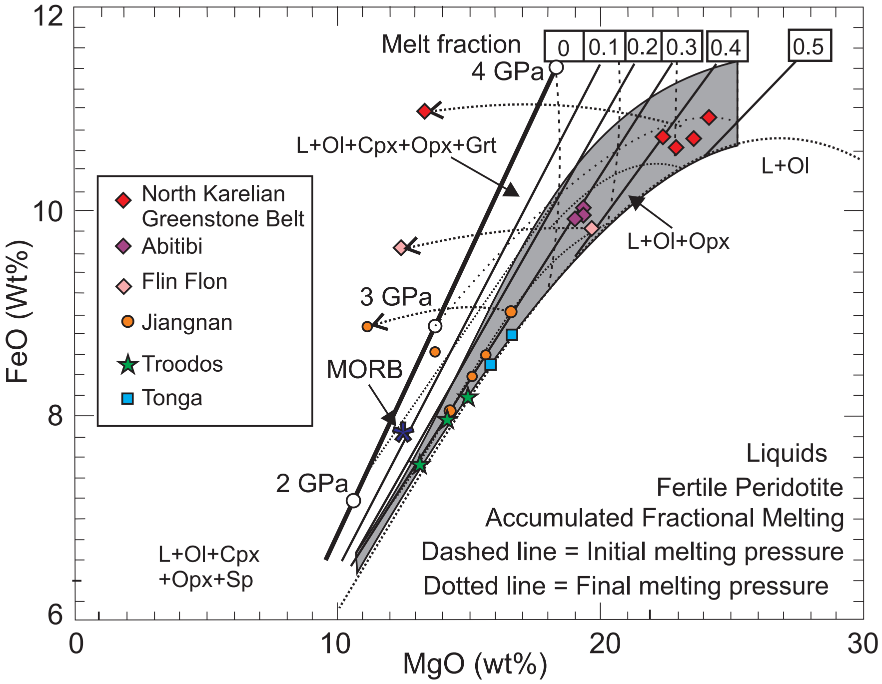

Fig. 8. Change in parental melts of boninite series compositions in time on the petrogenic grid MgO vs. FeO [*Herzberg, Asimow, 2008*].

Dotted curves with arrays are fractionation paths from the primary melts to evolved boninite compositions. Data source are for Tonga [*Falloon et al., 2008*]; Troodos [*Cameron, 1985*], Jiagnan [*Zhao, Asimow, 2014*]; Flin Flon [*Wyman, 1999a*]; Abitibi [*Kerrich et al., 1998*]; Iringora ophiolite, North Karelian greenstone belt [*Shchipansky et al., 2004*]. See the text for explanations.

Рис. 8. Изменение родительских составов бонинитовых серий во времени петрогенетической сетке MgO – FeO [*Herzberg, Asimow, 2008*].

Точечными кривыми со стрелками показаны тренды фракционирования от первичных расплавов к бонинитовым составам. Источники данных составов: Тонга [*Falloon et al., 2008*]; Троодос [*Cameron, 1985*], Цжэцзян [*Zhao, Asimow, 2014*]; Флин Флон [*Wyman, 1999a*]; Абитиби [*Kerrich et al., 1998*]; Ириногорские офиолиты Северо-Карельского пояса [*Shchipansky et al., 2004*]. См. объяснения в тексте.

presence of hydrous fluid. So, this phenomenon may be thought of as a result of the secular cooling of the Earth. The gradient of 50–70 °C/Ga suggests evolutionary changes in geodynamic processes in the Earth's history, rather than any significant transformations in tectonic mechanisms responsible for the continental crust growth. A nearly similar difference in the potential temperatures for the plume magmatism in the Earth's history is also noteworthy [*Herzberg et al., 2007*].

The evolution of boninitic volcanism in the Earth's history is clearly revealed in Figure 8 with regard to the definition of potential mantle temperature, envisaging a relationship between a mantle melting degree and a depth whereat the magma column is initiated due to decompression melting. The petrogenetic grid is used to show the calculated primary melt compositions of the Late Archean (North-Karelian and Abitibi belts), Paleoproterozoic (Flin Flon belt), Neoproterozoic (Jiangnan belt) and Meso-Cenozoic (Troodos, Tonga) boninite series, and a few fractionation trends are given for illustration of differentiation paths. It is clear that the early Precambrian boninite series were generated at higher degrees of mantle harzburgite melting (30–40 %), and the mantle melting columns occurred at considerably larger depths (3.5–4.0 GPa) than during the Phanerozoic eon (2.5–3.0 GPa). The knowledge of the P-T differences of the boninite series petrogenesis is important for understanding the evolution of geodynamic processes in the Earth's history that will be discussed below.

5. Geodynamic settings of boninite occurrence

Almost all the boninitic magmatism occurrences, regardless of its age, are genetically associated with intra-oceanic subduction zones (see Table 2). The modern boninitic volcanism occurrences revealed by the recent studies are localized only in the intra-oceanic plate convergence zones, and there is no proven example that would evidence any other geodynamic settings for their generation. Considerations of petrogenesis of the boninite series rock melts also imply their emplacement above the zones wherein the oceanic lithosphere slabs are dehydrating and sinking into the mantle. It is established that in the modern intraoceanic island arcs (Izu-Bonin-Mariana, and Tonga-Kermadec), the boninite series volcanic rocks build up the peridotite-gabbro sequences of the forearc slopes and indicate the initiation and growth of juvenile island-arcs [*Pearce et al.*, *1992*; *Stern, Bloomer*, *1992*; *Stern*, *2004*].

It should be noted that a genetic link between the boninite series and ophiolites was recognized well before the deep-sea drilling and dredging studies of the forearc slopes of the Tonga and Izu-Bonin-Mariana arcs [*Miyashiro*, *1973*; *Cameron et al.*, *1979*]. Numerous discoveries of the boninite series rocks [*Pearce*, *2003*, *2008*; *Stern*, *2004*; *Metcalf, Shervais*, *2008*; *Sklyarov et al.*, *2016*] have given grounds to conclude that the majority of the world's ophiolites mark paleo-zones of spreading in suprasubduction environments at the ancient oceanic plate margins, rather than past spreading at ancient mid-ocean ridges. Thus, boninites are petrologically unique rocks providing a perfect indication of paleogeodynamic settings in the oceanic plate convergence zones through the Earth's history.

The new paradigm of geodynamic settings for the boninite series generation was based on the hypothesis that SSZ ophiolites are related to the initiation of intra-oceanic island arcs [*Stern et al.*, *1991; Stern, Bloomer, 1992*]. This raised the questions of how and where subduction zones were initiated [*Stern*, *2002*, *2004*]. In terms of mechanics, a prerequisite for subduction initiation is gravitational instability in the oceanic lithosphere, which can lead to its tearing followed by decompression melting of the upper mantle and sinking of one plate under another. This phenomenon, as well as the genetic link between boninites and ophiolites, is encapsulated as the subduction initiation rule (SIR) [*Whattam, Stern*, *2011*].

In the model proposed in [*Stern*, *2004*], this condition is satisfied when plates of differing temperature and density are juxtaposed across a transform fault or fracture zone, i.e. theoretically, in case of the interaction between plates of different ages, i.e. an old cold plate and a young hot plate. Along the fault, the gravitationally instability of the ancient crust makes it sink with a down-dip component of motion, while a lateral component is lacking. The model suggest that upon initiation of sinking of the slab/plate, the overlying slab/plate is subject to stretching, the partially depleted mantle is rising to melt due to its decompression, and a large input of water from the sinking slab sets up conditions for extremely high extents of fusion. Later on, the slab motion vector acquires a lateral component, which stops the decompression, and, consequently, terminates melting of the depleted mantle. Thus, a true subduction regime is established for generation of the normal island-arc tholeiitic and calc-alkaline volcanic series.

Another subduction initiation concept is proposed in [*Niu et al.*, *2003*]. It establishes a link between locations of subduction zones and density inhomogeneities at the borders of the normal oceanic lithosphere and the oceanic lithosphere thickened by mantle plume impingement, i.e. oceanic plateaus or hotspot tracers – aseismic ridges or seamounts. This concept is supported by the data on the Tonga boninites that are confined to the intersection of the aseismic ridge of the Louisville hotspot and the paleotrough of the Tonga-Kermadec arc [*Turner, Hawkesworth*, *1997*]. There is also evidence that the initial stage of the Izu-Bonin-Mariana arc development was associated with mantle plume fingerprinting at the Manus back-arc basin [*Macpherson, Hall*, *2001*].

The boninite series volcanic rocks often have enriched mantle-plume isotopic and geochemical signatures [*Sobolev, Danyushevsky*, *1994*; *Taylor, Nesbitt*, *1998*]. The involvement of the mantle-plume thickened lithosphere in the petrogenesis of boninites would thus resolve the long debate on anomalously high temperatures for the initiation of partial melting of the depleted refractory mantle harzburgite as high heat inputs can be ensured by the ascending hot mantle plumes [*Falloon, Danyushevsky*, *2000*].

The presence of mantle-plume products is also revealed in the SSZ ophiolite sequences, which isotopic and geochemical compositions are well studied, such as the Pindos, Josephine, Koch, Magnitorsk (Southern Urals, Russia) ophiolites, etc. (see Table 2). In the early Precambrian sequences, the boninite series volcanic rocks are also associated with mantle-plume derivatives, komatiites, as well as OIB-type metavolcanic rocks [*Shchipansky*, *2008*].

Apparently, the occurrence of mantle-plume derivatives in the intra-oceanic subduction initiation zones does not seem to be random. It is recognized that a rising mantle plume can decrease the strength of the lithosphere, which may lead to the breakup of the continents [*Courtillot et al.*, *1999*]. In addition, an emplacement of mantle plume head at the lithosphere can significantly change its density characteristics. The ingress of melts generated by the enriched deep source into the upper layers of the mantle and the oceanic lithosphere would lead to refertilization of the previously depleted mantle. While cooling, the upper mantle transformed by mantle plume impingement becomes denser, and a new lithospheric segment may gradually become negatively buoyant. The reason is that OIB volcanic rocks are considerably enriched in Fe and Ti. Besides, Fe-Ti basalts/gabbros are known to being eclogitizated faster than their magnesium equivalents. Figure 9 shows the experimentally determined garnet stability fields for basalt compositions differing in

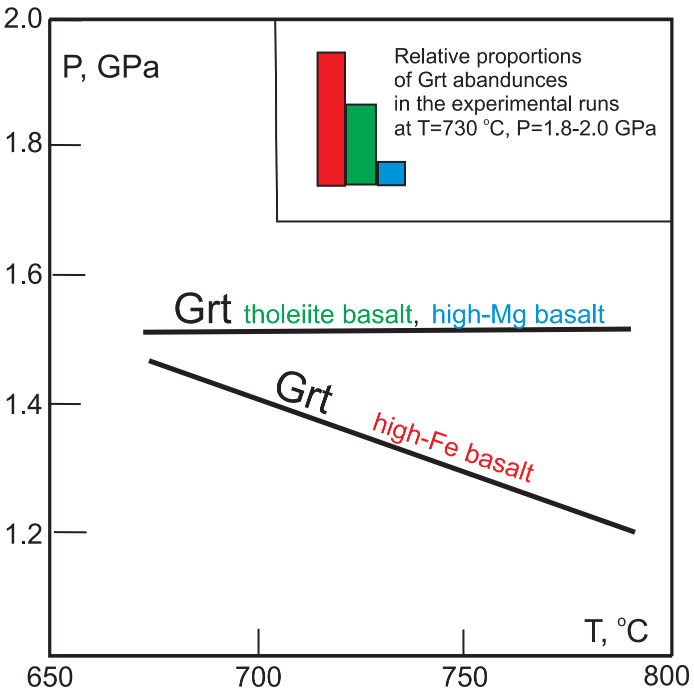

Fig. 9. Experimentally determined Grt-in curves for compositionally different basalts: Fe-rich basalt (Mg#=41), olivine tholeiite (Mg#=55), and high-Mg basalt (Mg#=69). Note that relative abundances of garnet shown at the inset vary significantly also. Modified after data of [*Molina, Poli, 2000*].

Рис. 9. Экспериментально определенные поля стабильности граната для базальтов различного состава: железистого базальта (Mg#=41), оливинового толеита (Mg#=55) и высокомагнезиального базальта (Mg#=69). Заметим, что относительные количества граната, показанные на врезке, также сильно варьируются. Модифицировано из работы [*Molina, Poli, 2000*].

magnesium numbers. Clearly, ferriferous compositions show the earliest occurrence of garnet in quantities considerably exceeding those in case of olivine tholeiites and, especially, high-Mg basalts. This metamorphic transformation at the crustal base of the thickened oceanic island builds seems to be a critical factor disturbing the gravitational stability of the lithosphere. Garnet is denser by almost 15 % than pyroxenes, amphiboles and olivine, which means that 'density eclogitization' can take place in the reworked lower lithosphere. In this case, even if only the lower crust is foundered, tearing of the lithosphere seems to be inevitable.

Actually, potential gravitational instability of the lithosphere seems to be directly dependent on a volume of the mantle-plume productivity and the thermal status of reworked lithosphere segment. It is not common that such factors are favorably combined; anyway, lithosphere breakup and initiation of new subduction zones is highly probable. It is noteworthy that the polarity of subduction is predetermined by the thermal status of the lithosphere – hot lithosphere is positively buoyant, while cold lithosphere is negatively buoyant.

The model in Figure 10 shows the global-scale chemical and density inhomogeneities of the lithosphere as a result of a superplume event. The term 'superplume' was coined by Roger Larson in the early 1990's, when the author has advocated that mantle-plume volcanism was the strongest in the mid-Cretaceous time (124–83 Ma) [*Larson, 1991*]. This event resulted in the emergence of giant oceanic plateaus, such as the Ontong Java, Manihiki, Kerguelen, and Columbia-Caribbean. It is believed that four currently active hotspots in the Pacific Ocean, which are traceable in the oceanic seafloor, are associated with this superplume. Few other tracks seem to have been cut off in the subduction zones. Other hotspot tracks in the Pacific are younger (Paleogene–Neogene) and may be not associated with deep plumes [*Clouard, Bonneville, 2001*]. Accordingly the numerical simulation of a termochemical superplume at the core–mantle boundary, protuberance emissions of the deep matter to the surface are represented by hot jets or large igneous provinces which impacts are observed even at the upper mantle [*Farnetani, Hofmann, 2011*]. This phenomenon may be responsible for the occurrence of the first-order chemical and density inhomogeneities and the initiation of the most extended plate convergence zones. This scenario seems to be realistic for the initiation of the Izu-Bonin-Mariana arc in the early Eocene.

Another subduction initiation scenario assumes a closer link between subduction and the geodynamics of individual hotspots. As already mentioned, the youngest boninitic magmatism occurrences in the northern Tonga are spatially associated with the Louisville hotspot track. Its forearc structure includes the Vitiaz paleo-trench (age of ~4 Ma) and the modern trench located further in the ocean at a distance of about 500 km. A unique double-subduction picture is revealed in this region by detailed seismotomographic surveys. A fragment of the younger and more gently dipping slab of the oceanic lithosphere is clearly visible above the current subduction zone [*Chen, Brudzinski, 2001*]. The shallow-depth slab detachment was discussed in detail in [*Shchipansky, 2008*] as the factor disturbing a lithospheric barrier and creating extremely favorable conditions for generation of the ophiolitic boninite series (Fig. 11).

It is quite possible that the shallow-depth slab break-off resulted from the compositional density inhomogeneity of the sinking lithosphere, such as local charging by OIB magmatism products. The key geodynamic implications of this phenomenon are, first, strong short-term thermal disturbance over the narrow slab window, and, second, fast uplift of its over-

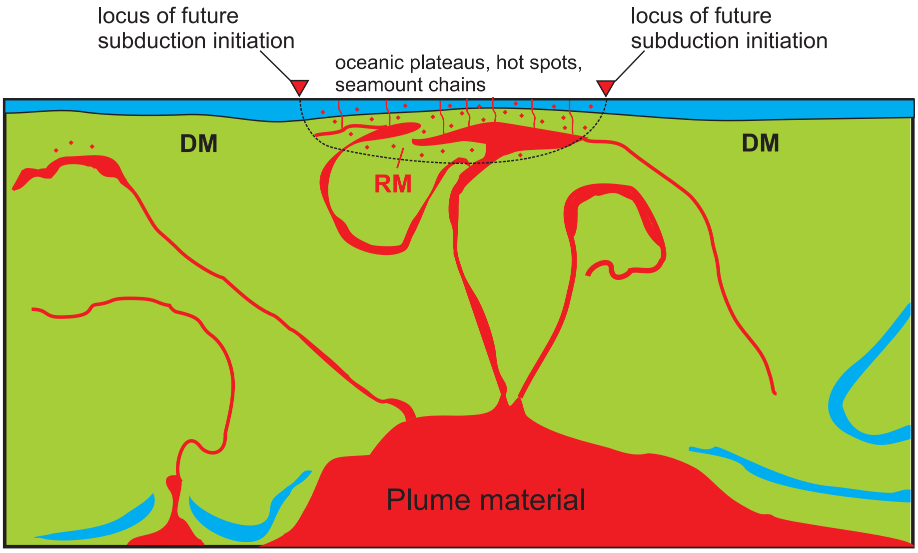

Fig. 10. Sketch illustrating an emergence of large refertilizited, or reworked, mantle (RM) region due to a superplume event.

This gives rise to a creation of lateral compositional buoyancy contrast over normal oceanic lithosphere (DM) and, thus, to a subduction initiation with time. Superplume cartoon is after the numerical simulation of a thermo-chemical plume [*Farnetani, Hofmann, 2011*].

Рис. 10. Схема, иллюстрирующая модель образования больших объемов рефертилизированной, или переработанной, мантии (RM) в результате суперплюмового события.

В результате со временем возникает химико-плотностной контраст по отношению к нормальной океанической литосфере (DM), что и определяет места инициации субдукции. Изображение суперплюма дано по результатам численного моделирования термохимического плюма [*Farnetani, Hofmann, 2011*].

riding plate [*van de Zedde, Wortel, 2001*; *Buiter et al., 2002*]. This mechanism provides a reasonable explanation for the short-term (3–5 Ma) volcanism which was by far more voluminous that the steady-state subduction volcanism [*Stern, 2002, 2004*]. Due to uplifting of the suprasubduction plate, an ophiolite 'platform' replaced the hanging plate and provided a basement for the nascent island-arc build. It is essential that the uplift of the ophiolite 'platform' could have attained the morphological stability as the previous episode of

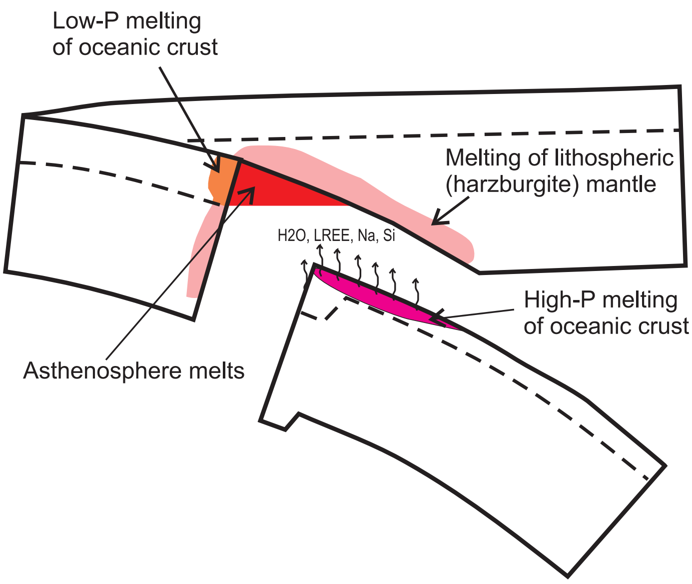

Fig. 11. Cartoon depicting a variety of the partial melting processes during shallow-level slab break-off [*Shchipansky, 2008*].

Note that in this case different portions of the upper mantle, i.e. lherzolitic asthenospheric and harzburgitic lithospheric, should be partially molten. Crustal part of the detached slab provides a source for aqueous fluids enriched by subduction-related chemical components. Loci of low pressure and high pressure melting of metabasic oceanic rocks are shown also.

Рис. 11. Принципиальная схема процессов частичного плавления в обстановке малоглубинного детачмента слэба. Модифицировано из работы [*Shchipansky, 2008*].

Обратим внимание, что в этом случае в область плавления включаются различные составляющие верхней мантии – лерцолитовая астеносферная мантия, гарцбургитовая литосферная мантия. Коровая часть оторванного слэба является поставщиком водного флюида и субдукционной компоненты. Показаны также вероятные области низкобарического и высокобарического (адакитового) плавления метабазитов океанической коры.

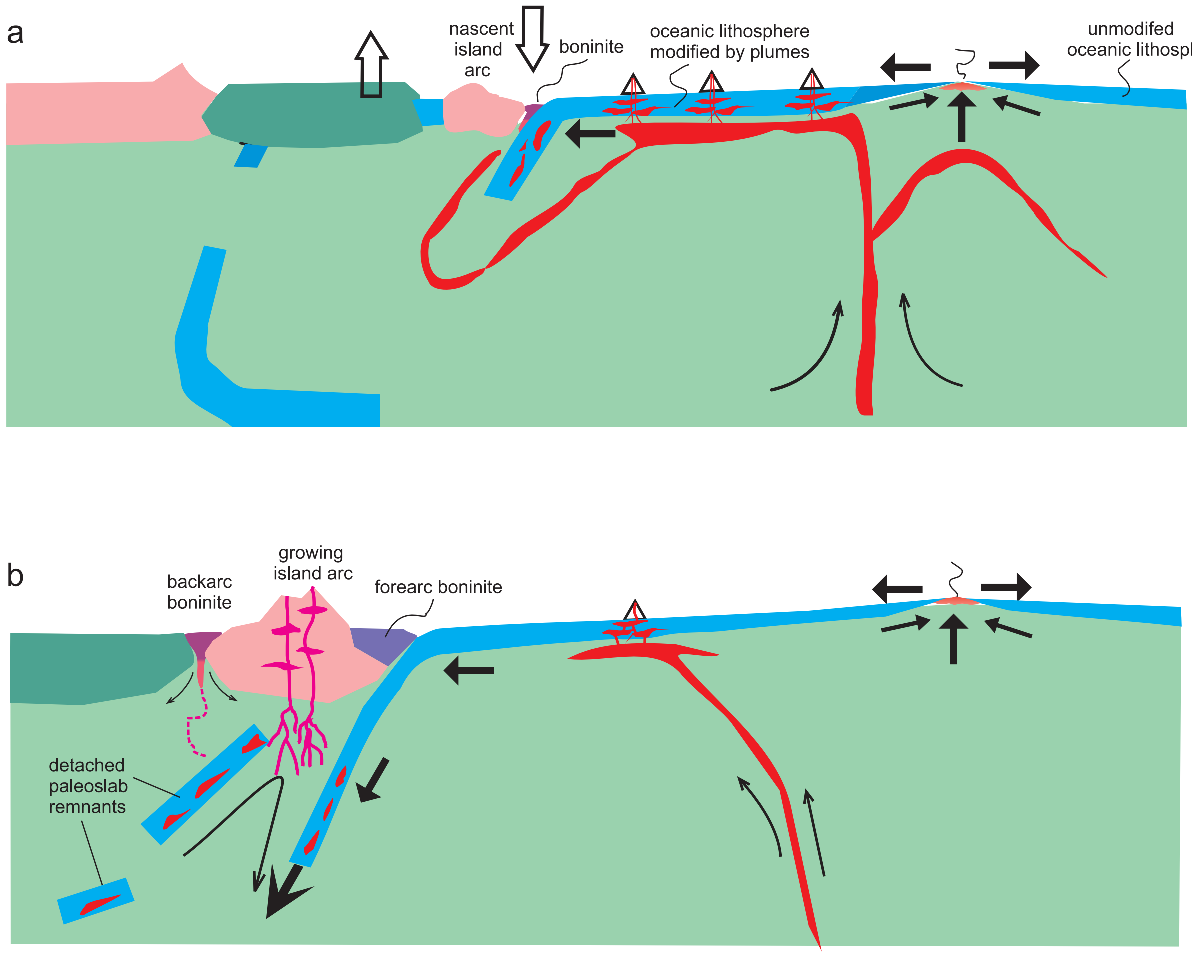

Fig. 12. An illustration of the model of boninite formation when a reworked lithosphere caped by OIB volcanics initiates a non-stationary subduction.

The model is largely based on the available data from the modern Tonga arc [*Sobolev, Danyushevsky, 1994; Turner, Hawkesworth, 1997; Chen, Brudzinski, 2001; Niu et al., 2003; Falloon et al., 2007, 2008; Resing et al., 2011*]: *a* – lithosphere charged with Fe-rich melts gets negative buoyancy as it cooled, and starts to sink. Lithosphere tearing leads to raise asthenospheric mantle and triggers intensive melting that includes boninite series melts (see fig. 10); *b* – as a result of the shallow level slab break-off, a new subduction should develop and, as a consequence, a new trench occurs at a distance of a few hundred kilometers oceanward from the older trench. Detached slab fragments lead to a lithosphere extension, thus forming a tight back-arc trough characterized by occurrences of local multi-spreading centers where younger boninites can also be formed. See the text for more details.

Рис. 12. Иллюстрация модели формирования бонинитов подразумевающей инициацию нестационарной субдукции при участии переработанной и нагруженной OIB вулканитами литосферы.

Модель основана на многочисленных данных по современной островной дуге Тонга [*Sobolev, Danyushevsky, 1994; Turner, Hawkesworth, 1997; Chen, Brudzinski, 2001; Niu et al., 2003; Falloon et al., 2007, 2008; Resing et al., 2011*]. *a* – литосфера, отягощенная богатыми железом расплавами, по мере охлаждения приобретает отрицательную плавучесть и начинает погружаться. Разрыв литосферы приводит к подъему астеносферной мантии и вызывает интенсивное плавление, включая генерацию магм бонинитовой серии (см. рис. 10); *b* – в результате малоглубинного обрыва слэба возникает новая зона субдукции, новый желоб которой располагается на расстоянии в несколько сотен километров в сторону океана от предшествующего желоба. Оторванные фрагменты палеослэба провоцируют растяжение литосферы, что вызывает формирование узкого задугового трога, характеризующегося развитием мульти-спрединговых центров, где могут формироваться более молодые бониниты. См. текст для более детальной информации.

intense mantle melting leaved the mantle strongly depleted. This resulted in the emergence of a lithospheric keel capable to resist the convective instability of the surrounding mantle.

Figure 12 shows the above-described model based on the modern geodynamics of the northern termination of the Tonga arc. The top panel shows the subduction initiation and generation of boninites in the forearc region. The bottom panel shows the modern subduction zone and paleoslab fragments under the emerging Lau basin. In the samples dredged from the Lau basin, the presence of the subduction fluid component is evidenced by higher contents of H_2O in glasses and enrichment in large-ion lithophile (LIL) elements [*Falloon et al.*, *1992*; *Danushevsky et al.*, *1993*; *Pearce et al.*, *1994*]. The fact that compositions of these basalts significantly differ can be explained by contribution to their petrogenesis of various mantle sources, including mantle plume input. Besides, active eruptions of boninites take place at present time [*Resing et al.*, *2011*]. Thus, boninites occur in a variety of combinations in different tectonic settings in time and space, i.e. in the fore- and back-arc environments. This indicates that, firstly, it is an established phenomenon, and, secondly, the subduction initiation process may be not as simple as described by the 'subduction initiation rule' (SIR) model [*Whattam, Stern*, *2011*].

It seems likely that the subduction regime should be stabilized after a certain period of accommodation associated with the slab break-off event/ or events and resultant contrasting tectonic regimes on the surface. During this period, movements caused by the frontal subduction compression are rapidly replaced by strike-slip motion, which leads to the occurrence of a complex rift system with both hot spot volcanism and volcanic seamounts [*Falloon et al.*, *2007*, *2008*].

Considering the ophiolite sequences worldwide, it has been noted that, although their magmatic chemostratigraphic progression is almost similar [*Pearce, Robinson*, *2010*; *Whattam, Stern*, *2011*], the relationship between boninite series and other members of ophiolite sections are variable and may significantly differ from the ideal ophiolite sequence, known as a 'penrose ophiolite' [*Sklyarov et al.*, *2016*]. In the literature, there are numerous cases showing the lateral variability of the ophiolite sequences within the local regions and therefore suggests non-stationary settings of ophiolite-forming processes. These increasingly compel the conclusion that ophiolites are commonly associated with the subduction initiation environments, rather than with spreading in the mid-ocean ridges.

6. Subduction initiation in the Early Precambrian

As described above, generation of the early Precambrian boninite series was developed by mantle harzburgite melting of high degrees (30–40 %), and the mantle melt columns started at greater depth (3.5–4.0 GPa) as comparing with those from Phanerozoic eon (2.5–3 GPa). What are the geodynamic implications of these facts?

It is well known that the early Precambrian cratons are underlain by the depleted subcontinental lithospheric mantle (SCLM) or a lithospheric keel (root) extending into the diamond stability field. This phenomenon has never reoccurred in the later history of the Earth, and its origin has been widely discussed in the literature [e.g. *Herzberg, Rudnick*, *2012*; *Shchipansky*, *2012*, *and references therein*]. In the Phanerozoic, strong depletion of the upper mantle is associated with generation of the boninite series in the subduction initiation zones. The above overview of the global boninite occurrences gives abundant evidence of boninitic magmatism in the early Precambrian, and the discoveries of ancient boninites are progressively growing. Accordingly to the recently published assessment, the volumes of the Archean boninite volcanics and komatiites appear to be almost roughly similar (Fig. 13) [*Furnes et al.*, *2014*]. Discovery of the boninite series rocks with fragments of sheeted dikes and IAT-type metabasites in the oldest preserved complex Isua strongly suggests that subduction dates back from the early Earth's geological history.

A prerequisite for subduction initiation is the oceanic lithosphere breakup through its entire thickness. It follows thus from Figure 6 that, first, the early Precam-

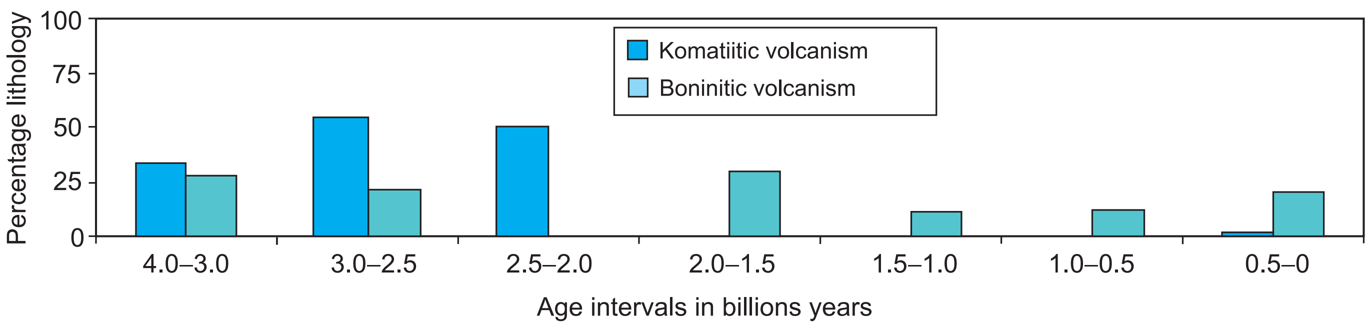

Fig. 13. Percentage lithology of komatiite and boninitic volcanism represented at given age intervals, relative to total of mafic and ultramafic magmatism in the Earth history, according to [*Furnes et al., 2014*].

Рис. 13. Соотношения объемов коматиитового и бонинитового вулканизма в процентах от общего объема мафит-ультрамафитовых ассоциаций в истории Земли, по [*Furnes et al., 2014*].

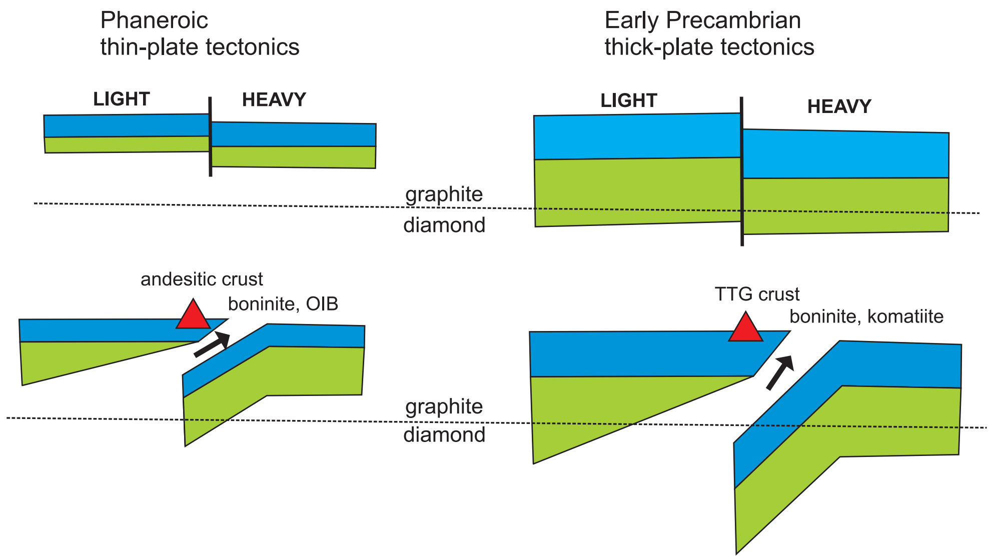

Fig. 14. Sketch illustrating distinctions between subduction initiations in modern thin-plate and Early Precambrian thick-plate tectonic settings. The dotted lines depict a conventional graphite/graphite transition relative to lithospheric mantle.

Рис. 14. Схема, иллюстрирующая различия в инициации субдукции, в обстановках современной тонкоплитовой и раннедокембрийской толстоплитовой тектоники. Точечной линией условно показано положение фазового перехода графит/алмаз относительно литосферной мантии.

brian lithosphere as a unit should have rheological properties providing for brittle or brittle-plastic deformations. In other words, such lithosphere can be considered as a rigid body capable of resisting the convective instability that is an attribute of plate tectonics [*Sleep*, *1992*]. The Archaean oceanic lithosphere thickness is estimated at 85–120 km, whereas the modern lithosphere is ~60 km thick [*Herzberg et al.*, *2010*].

Second, unlike the Phanerozoic boninite series, parental melts of the early Precambrian series were generated at depths of ~120–130 km, i.e. in the diamond stability field. Given the fact that the primitive melts of the ancient boninite series clearly have the subduction influence signatures, it is reasonable to believe that deep sinking of the slabs into the early Precambrian mantle was highly possible.

Third, extensive melting of the early Precambrian upper mantle for the period of subduction initiation implies that it was subject to strong depletion through the diamond stability field. During the accommodation stage, the new sinking slab/slabs are cut off the asthenospheric heat input thus leading to quickly cooling of overriding forearc lithosphere. This model provides an explanation of the origin and stability of the cold diamond-bearing SCLM that has not been subject to any convective perturbations, at least, since 3.0 billion years [*Boyd et al.*, *1985*].

The differences between the modern and early Precambrian subduction initiation settings are schematically shown in Figure 14. The main distinction is that thin-plate tectonics covers the period from the Neoproterozoic to the present time, and thick-plate tectonics refers to the early Precambrian. Today, the oceanic crust is ~6–7 km thick on average, and this requires ~6–7 % melting. In general, about 1 km of oceanic crust is produced for every 1 % of partial melting (i.e. 1 km/1 % melting) [*Herzberg, Rudnick*, 2012]. According to available petrological estimations, the Archean MORB-type oceanic crust thickness ranges from ~20–25 km [*Abbott et al.*, *1994*] to 40–60 km [*Herzberg et al.*, *2010*]. In other words, the Archaean oceanic crust should have been, roughly, 3 to 6 times thicker than the modern crust. Such estimations scatter is due to the problem of validity of mantle potential temperature (*Tp*) computations for the ambient Archaean upper mantle as preserved off-arcs mafic volcanics of that age are very seldom [*Pearce*, *2008; and others*].

Anyway, thickening of the Archean oceanic crust is a prerequisite for generation of tonalite–trondhjemite–granodiorite (TTG) gneisses composing the bulk Archean continental crust. Both tonalite granitoids and their high-pressure analogues (adakites) are observed in modern suprasubduction settings, although in much smaller amounts than the basalt–andesite–rhyolite series.

7. Conclusion

The boninite series and its most fractionated end-member, boninites, are not just a simple unit of the suprasubduction sequence, but also a vivid indicator of initiation of intra-oceanic convergence zones. Being directly related to ophiolites, boninites and low-Ti basalts/picrites give direct evidence that the oceanic lithosphere stretching was related to subduction initiation. This means that the age of SSZ ophiolites or, more precisely, SIR ophiolites [*Whattam, Stern*, *2011*] may show the age of paleo-oceans only in the first approximation. The oceanic lithosphere itself may be much older. Indeed, the modern boninites of the northern Tonga arc, the Eocene IBM boninites and ophiolites of Papua New Guinea cannot evidently correspond to timing of the Pacific or Indo-Austarlian plate life. Moreover, the Phanerozoic folded belts show multi-suturation signatures rather than mono-suture architecture.

The records of MOR-type ophiolites are very seldom as comparing with the large occurrences of the SIR ophiolites including the well-known sequences of Troodos, Semail, or Newfoundland [*Shervais, 2001; and others*]. The completely developed MOR-type includes ophiolites of 12–9 Ma age in the Macquarie Island located at the boundary between the Pacific and Australian plates, and the Neoproterozoic ophiolites of Gabal Gerf, the Arab-Nubian shield [*Pearce*, *2008*; *Whattam, Stern*, *2011*, and references therein]. A rarity of the MOR type in the ophiolite continuum stems well from the fact that physically it is almost impossible to emplace true MORB crust at a convergent plate boundary; rather sediments and fragments of seamounts may be scraped off of the sinking plate [*Stern*, *2004*].

It is now recognized that SIR ophiolites are volumetrically major in the Earth's geological history (see Table 2 and [*Furnes et al*., *2014*]). As shown above, a prerequisite for subduction initiation is a lateral compositional buoyancy contrast within the lithosphere which would led to its collapse and consequently to form zones of intra-oceanic plate convergence. An impingement of mantle plume into the pre-existing lithosphere appears to be the most obvious among the known mechanisms controlling the global geodynamics of the Earth. However, mantle plumes themselves do not seem to be responsible for continental crust growing, even in the case of Iceland plateau placed directly above the hot mantle plume head [*Martin et al*., *2008*]. However recently subducted oceanic plateaus crust revealed the capability to produce a juvenile continental crust similar to Archean TTG via its partial hydrous melting [*Hastie et al*., *2010*]. It is vital also, that high-pressure adakites are also found in association with the Tonga boninites related to the hot spot track [*Falloon et al*., *2008*]. Furthermore, the mere fact that boninites tend to be compositionally close to the bulk composition of continental crust suggesting that the crustal growth processes began with the subduction initiation (see Fig. 3).

Thus, lacking direct influence on crustal growing at the intra-oceanic island-arc zones, mantle plume events could have acted as ‘remote triggers’ of theses process and predetermined subsequent loci of subduction initiation zones. Such a kind of the self-organized geodynamic system of the Earth may have originated as early as Eoarchean, and its further evolution was mainly operated by the secular cooling of the planet.

8. Acknowledgements

This work is a contribution to National Task 01201459184. It was also supported by Grant 16-05-00479 of the Russian Foundation for Basic Research.

9. References

Abbott D.H., Burgess L., Longhi J., Smith W.H.F., 1994. An empirical thermal history of the Earth`s upper mantle. *Journal of Geophysical Research* 99 (B7), 13835–13850. http://dx.doi.org/10.1029/94JB00112.

Aitchison J.C., Ireland T.R., Clarke G.L., Cluzel D., Davis A.M., Meffre S., 1998. Regional implications of U/Pb SHRIMP age constraints on the tectonic evolution of New Caledonia. *Tectonophysics* 299 (4), 333–343. http://dx.doi.org/10.1016/S0040-1951(98)00211-X.

Angerer T., Kerrich R., Haggemann S.G., 2013. Geochemistry of a komatiitic, boninitic, and tholeiitic basalt assotiation in the Mesoarchean Koolyanobbing greenstone belt, Southern Cross Domain, Yilgarn craton: Implications for mantle source and geodynamic settings of banded iron formation. *Precambrian Research* 224, 110–128. http://dx.doi.org/10.1016/j.precamres.2012.09.012.

Arculus R.J., Pearce J.A., Murton B.J., van der Laan S.R., 1992. Igneuos stratigraphy and major-element geochemistry of holes 786A and 786B. In: P. Fryer, P. Coleman, J.A. Pearce, L.B. Stokking (Eds.), Proceedings of the Ocean Drilling Program, Scientific Results, vol. 125, p. 143–169. http://dx.doi.org/10.2973/odp.proc.sr.125.137.1992.

Bédard J.H., 1999. Petrogenesis of boninites from the Betts Cove ophiolite, Newfoundland, Canada: identification of subducted source components. *Journal of Petrology* 40 (12), 1853–1889. http://dx.doi.org/10.1093/petroj/40.12.1853.

Bédard J.H., Lanzière K., Tremblay K., Sangster A., 1998. Evidence for forearc sea-floor spreading from the Betts Cove ophiolite, Newfoundland: oceanic crust of boninitic affinity. *Tectonophysics* 284 (3–4), 233–245. http://dx.doi.org/10.1016/S0040-1951(97)00182-0.

Belova A.A., Ryazantsev A.V., Razumovsky A.A., Degtyarov K.E., 2010. Early Devonian suprasubduction othiolites of the Southern Urals. *Geotectonics* 44 (4), 321–343. http://dx.doi.org/10.1134/S0016852110040035.

Bibikova E.V., Samsonov A.V., Shchipansky A.A., Bogina M.M., Gracheva T.V., Makarov V.A., 2003. The Hisovaara structure in the northern Karelian greenstone belt as a Late Archean accreted island arc: isotopic geochronological and petrological evidence. *Petrology* 11 (3), 261–290.

Bloomer S.H., Taylor B., MacLeod C.J., Stern J.R., Fryer P., Hawkins J.W., Johnson L., 1995. Early arc volcanism and the ophiolite problem: a perspective from drilling in the western Pacific. In: B. Taylor, J.H. Natland (Eds.), Active margins and marginal basins of the Western Pacific. AGU Geophysical Monograph Series, vol. 88, p. 1–30. http://dx.doi.org/10.1029/GM088p0001.

Boily M., Dion C., 2002. Geochemistry of boninite-type volcanic rocks in the Frotet-Evans greenstone belt, Opatica subprovince, Quebec: implications for the evolution of Archaean greenstone belts. *Precambrian Research* 115 (1–4), 349–371. http://dx.doi.org/10.1016/S0301-9268(02)00016-5.

Bortolotti V., Kodra A., Marroni M., Mustafa F., Pandolfi L., Principi G., Saccani E., 1996. Geology and petrology of ophiolitic sequences in the Mirdita region (northern Albania). *Ofioliti* 21 (1), 3–20.

Bortollotti V., Marroni M., Pandolfi L., Principi G., Saccani E., 2002. Interaction between mid-ocean ridge and subduction magmatism in Albanian ophiolites. *The Journal of Geology* 110 (5), 561–576.

Boyd F.R., Gurney J.J., Richardson S.H., 1985. Evidence for a 150–200 km thick Archean lithosphere from diamond inclusion thermobarometry. *Nature* 315 (6018), 387–389. http://dx.doi.org/10.1038/315387a0.

Brown A.V., Jenner G.A., 1989. Geological setting, petrology and geochemistry of Cambrian boninite and low-Ti tholeiite lavas in Western Tasmania. In: A.J. Crawford (Ed.), Boninites and related rocks. Unwin Human, London, p. 232–263.

Builter S.J.H., Govers R., Wortel M.J.R., 2002. Two-dimentional simulations of surface deformation caused by slab detachment. *Tectonophysics* 354 (3–4), 195–210. http://dx.doi.org/10.1016/S0040-1951(02)00336-0.

Cameron W.E., 1985. Petrology and origin of primitive lavas from the Troodos ophiolite, Cyprus. *Contributions to Mineralogy and Petrology* 89 (2), 239–255. http://dx.doi.org/10.1007/BF00379457.

Cameron W.E., Nisbet E.G., Dietrich V.J., 1979. Boninites, komatiites and ophiolitic basalts. *Nature* 280 (5723), 550–553. http://dx.doi.org/10.1038/280550a0.

Cameron W.E., Nisbet E.G., Dietrich V.J., 1980. Petrographic dissimilarities between ophiolitic and ocean floor basalts. In: A. Panayiotou (Ed.), Ophiolites: Proceedings of the International Ophiolite Symposium. Geological Survey of Cyprus, Nicosia, Cyprus, p. 182–192.

Cawood P.A., Hawkesworth C.J., 2014. Earth's middle age. *Geology* 42 (6), 503–506. http://dx.doi.org/10.1130/G35402.1.

Chen W.-P., Brudzinski M., 2001. Evidence for a large-scale remnant of subducted lithosphere beneath Fiji. *Science* 292 (5526), 2475–2479. http://dx.doi.org/10.1126/science.292.5526.2475.

Clouard V., Bonneville A., 2001. How many Pacific hotspots are fed by deep-mantle plumes? *Geology* 29 (8), 695–698. http://dx.doi.org/10.1130/0091-7613(2001)029<0695:HMPHAF>2.0.CO;2.

Courtillot V.E., Jaupart C., Manighetti I., Tapponier P., Besse J., 1999. On causal links between flood basalts and continental breakup. On causal links between flood basalts and continental breakup. *Earth and Planetary Science Letters* 166 (3–4), 177–195. http://dx.doi.org/10.1016/S0012-821X(98)00282-9.

Crawford A.J., Beccaluva L., Serri G., 1981. Tectono-magmatic evolution of the West Philippine-Mariana region and the origin of boninites. *Earth and Planetary Science Letters* 54 (2), 346–356. http://dx.doi.org/10.1016/0012-821X(81)90016-9.

Crawford A.J., Beccaluva L., Serri G., Dostal J., 1986. Petrology, geochemistry and tectonic implications of volcanics dredged from the intersection of the Yap and Mariana trenches. *Earth and Planetary Science Letters* 80 (3–4), 265–280. http://dx.doi.org/10.1016/0012-821X(86)90110-X.

Crawford A.J., Berry R.F., 1992. Tectonic implications of Late Proterozoic – Early Palaeozoic igneous rock associations in western Tasmania. *Tectonophysics* 214 (1–4), 37–56. http://dx.doi.org/10.1016/0040-1951(92)90189-D.

Crawford A.J., Cameron W.E., 1985. Petrology and geochemistry of Cambrian boninites and low-Ti andesites from Heathcote, Victoria. *Contributions to Mineralogy and Petrology* 91 (1), 93–104. http://dx.doi.org/10.1007/BF00429431.

Crawford A.J., Fallon T.J., Green D.H., 1989. Classification, petrogenesis and tectonic setting of boninites. In: A.J. Crawford (Ed.), Boninites and related rocks. Unwin Hyman, London, p. 2–44.

Danushevsky L.V., Fallon T.J., Sobolev A.V., Crawford A.J., Carroll M., Price R.C., 1993. The H_2O content of basalt glasses from southwest Pacific back-arc basins. *Earth and Planetary Science Letters* 117 (3–4), 347–362. http://dx.doi.org/10.1016/0012-821X(93)90089-R.

De Wit M.J., Ashwal L.D., 1997. Convergence towards divergent models of greenstone belts: In: M. de Wit, L.D. Ashwal (Eds.), Greenstone belts. Oxford Monographs on Geology and Geophysics, vol. 35, p. x–xii.

Dobretsov N.L., Konnikov E.G., Sklyarov E.V., Medvedev V.N., 1986. Marianite-boninite series and evolution of ophiolite magmatism of East Sayan. *Geologiya i Geofizika* (*Soviet Geology and Geophysics*) (12), 29–35 (in Russian) [*Добрецов Н.Л., Конников Э.Г., Скляров Е.В., Медведев В.Н.* Марианит-бонинитовая серия и эволюция офиолитового магматизма Восточного Саяна // *Геология и геофизика*. 1986. № 12. С. 29–35].

Dobretsov N.L., Simonov V.A., Buslov M.M., Kotlyarov A.V., 2005. Magmatism and geodynamics of the Paleoasian ocean at the Vendian-Cambrian stage of its evolution. *Geologiya i Geofizika* (*Russian Geology and Geophysics*) 46 (9), 933–951.

Duncan R.A., Green D.H., 1980. Role of multistage melting in the formation of oceanic crust. *Geology* 8 (1), 22–26. http://dx.doi.org/10.1130/0091-7613(1980)8<22:ROMMIT>2.0.CO;2.

Duncan R.A., Green D.H., 1987. The genesis of refractory melts in the formation of oceanic crust. *Contributions to Mineralogy and Petrology* 96 (3), 326–342. http://dx.doi.org/10.1007/BF00371252.

Falloon T.J., Crawford A.J., 1991. The petrogenesis of high-calcium boninite lavas dredged from the northern Tonga ridge. *Earth and Planetary Science Letters* 102 (3–4), 375–394. http://dx.doi.org/10.1016/0012-821X(91)90030-L.

Falloon T.J., Danyushevsky L.V., 2000. Melting of refractory mantle at 1.5, 2 and 2.5 GPa under anhydrous and H_2O-undersaturated conditions: Implications for the petrogenesis of high-Ca boninites and the influence of subduction components on mantle melting. *Journal of Petrology* 41 (2), 257–283. http://dx.doi.org/10.1093/petrology/41.2.257.

Falloon T.J., Danyushevsky L.V., Crawford T.J., Maas R., Woodhead J.D., Eggins S.M., Bloomer S.H., Wright D.J., Zlobin S.K., Stacey A.R., 2007. Multiple mantle plume components involved in the petrogenesis of subduction related lavas from the northern termination of the Tonga Arc and northern Lau Basin: evidence from the geochemistry of arc and backarc submarine volcanics. *Geochemistry, Geophysics, Geosystems* 8 (9), Q09003. http://dx.doi.org/10.1029/2007GC001619.

Falloon T.J., Danyushevsky L.V., Crawford A.J., Meffre S., Woodhead J.D., Bloomer S.A., 2008. Boninites and adakites from the Northern termination of the Tonga trench: implications of adakite petrogenesis. *Journal of Petrology* 49 (4), 697–715. http://dx.doi.org/10.1093/petrology/egm080.

Falloon T.J. Malahoff A., Zonenshain L.P., Bogdanov Y., 1992. Petrology and geochemistry of back-arc basin basalts from Lau Basin spreading ridges at 15°, 18° and 19°S. *Mineralogy and Petrology* 47 (1), 1–35. http://dx.doi.org/10.1007/BF01165295.

Farnetani C.G., Hofmann A.W., 2011. Mantle Plumes. In: H.K. Gupta (Ed.), Encyclopedia of Solid Earth geophysics. Springer, Dordrecht, p. 857–869. http://dx.doi.org/10.1007/978-90-481-8702-7_132.

Furnes H., Dilek Y., de Wit M., 2015. Precambrian greenstone sequences represent different ophiolite types. *Gondwana Research* 27 (2), 649–685. http://dx.doi.org/10.1016/j.gr.2013.06.004.

Furnes H., Rosing M., Dilek Y., de Wit, 2009. Isua supracrustal belt (Greenland) – a vestige of a 3.8 Ga suprasubduction zone ophiolite, and the implications for Archean geology. *Lithos* 113 (1–2), 115–132. http://dx.doi.org/10.1016/j.lithos.2009.03.043.

Furnes H., de Wit M., Staudigel H., Rosing M., Muenhlenbachs K., 2007. A vestige of Earth's oldest ophiolite. *Science* 315 (5819), 1704–1707. http://dx.doi.org/10.1126/science.1139170.

Furnes H., de Wit M., Dilek Y., 2014. Four billion years of ophiolites reveal secular trends in oceanic crust formation. *Geoscience Frontiers* 5 (4), 571–603. http://dx.doi.org/10.1016/j.gsf.2014.02.002.

Ganelin A.V., Silantjev S.A., 2008. Composition and geodynamic conditions of formation of the intrusive rocks of the Gromadnen-Vurguveem peridotite-gabbro massif, western Chukotka. *Petrology* 16 (6), 565–583. http://dx.doi.org/10.1134/S0869591108060039.

Hall R.P., Hughes D.J., 1993. Early Precambrian crustal development: changing styles of mafic magmatism. *Journal of the Geological Society* 150 (4), 625–635. http://dx.doi.org/10.1144/gsjgs.150.4.0625.

Harper G.D., 1984. The Josephine Ophiolite, northwestern California. *Geological Society of America Bulletin* 95 (9), 1009–1026. http://dx.doi.org/10.1130/0016-7606(1984)95<1009:TJONC>2.0.CO;2.

Harper G.D., 2003. Fe-Ti basalts and propagating-rift tectonics in the Josephine Ophiolite. *Geological Society of America Bulletin* 115 (7), 771–787. http://dx.doi.org/10.1130/0016-7606(2003)115<0771:FBAPTI>2.0.CO;2.

Hastie A., Kerr A.C., McDonald I., Mitchell S.F., Pearce J.A., Wolstencroft M., Millar I.L., 2010. Do Cenozoic analogues support a plate tectonic origin for Earth's earliest continental crust? *Geology* 38 (6), 495–498. http://dx.doi.org/10.1130/G30778.1.

Herzberg C., Asimow P., 2008. Petrology of some Oceanic Island Basalts: PRIMELT2.XLS software for Primary Magma Calculation. *Geochemistry, Geophysics, Geosystems* 9 (9), Q09001. http://dx.doi.org/10.1029/2008GC002057.

Herzberg C., Asimow P., Arndt N., Niu Y., Lesher C.M., Fitton J.G., Cheadle M.G., Saunders A.D., 2007. Temperatures in ambient mantle and plumes: Constraints from basalts, picrites, and komatiites. *Geochemistry, Geophysics, Geosystems* 8 (2), Q02006. http://dx.doi.org/10.1029/2006GC001390.

Herzberg C., Condie K., Korenaga J., 2010. Thermal history of the Earth and its petrological expression. *Earth and Planetary Science Letters* 292 (1–2), 79–88. http://dx.doi.org/10.1016/j.epsl.2010.01.022.

Herzberg C., Rudnick R., 2012. Formation of cratonic lithosphere: an integrated thermal and petrological model. *Lithos* 149, 4–15. http://dx.doi.org/10.1016/j.lithos.2012.01.010.

Hickey R.L., Frey F.A., 1982. Geochemical characteristics of boninite series volcanics: Implications for their source. *Geochimica et Cosmochimica Acta* 46 (11), 2099–2115. http://dx.doi.org/10.1016/0016-7037(82)90188-0.

Hofmann A.W., 1988. Chemical differentiation of the Earth: The relationship between mantle continental crust and oceanic crust. *Earth and Planetary Science Letters* 90 (3), 297–314. http://dx.doi.org/10.1016/0012-821X(88)90132-X.

Ishikawa T., Nagaishi K., Umino S., 2002. Boninitic volcanism in the Oman ophiolite: Implications for thermal condition during transition from spreading ridge to arc. *Geology* 30 (10), 899–902. http://dx.doi.org/10.1130/0091-7613(2002)030<0899:BVITOO>2.0.CO;2.

Kepezhinskas P.K., Kepezhinskas K.B., Puchtel I.S., 1991. Lower Paleozoic oceanic crust in Mongolian Caledonides: SM-ND isotope and trace element data. *Geophysical Research Letters* 18 (7), 1301–1304. http://dx.doi.org/10.1029/91GL01643.

Kerrich R., Wyman D., Bleeker W., 1998. Boninite series: low Ti-tholeiite associations from the 2.7 Ga Abitibi greenstone belt. *Earth and Planetary Science Letters* 164 (1–2), 303–316. http://dx.doi.org/10.1016/S0012-821X(98)00223-4.

Khain E.V., Bibikova E.V., Kröner A., Zhuravlev D.Z., Sklyarov E.V., Fedotova A.A., Kravchenko-Berezhnoy I.R., 2002. The most ancient ophiolite of the Central Asian fold belt: U-Pb and Pb-Pb zircon ages for the Dunzhugur Complex, Eastern Sayan, Siberia, and geodynamic implications. *Earth and Planetary Science Letters* 199 (3–4), 311–325. http://dx.doi.org/10.1016/S0012-821X(02)00587-3.

Khain E.V., Bibikova E.V., Salnikova E.B., Kröner A., Gibsher A.S., Didenko A.N., Degtyarev K.E., Fedotova A.A., 2003. The Palaeo-Asian ocean in the Neoproterozoic and early Palaeozoic: new geochronologic data and palaeotectonic reconstructions. *Precambrian Research* 122 (1–4), 329–358. http://dx.doi.org/10.1016/S0301-9268(02)00218-8.

Kosarev A.M., Puchkov V.N., Seravkin I.B., 2005. Petrological and geochemical features of the Early Devonian – Eifelian island-arc volcanics of the Magnitogorsk zone in a geodynamic context. *Litosfera* (*Lithosphere*) (4), 22–41 (in Russian) [*Косарев А.М., Пучков В.Н., Серавкин И.Б.* Петролого-геохимические особенности раннедевонско-эйфельских островодужных вулканитов магнитогорской зоны в геодинамическом контексте // *Литосфера*. 2005. № 4. С. 22–41].

Kushiro I., 1990. Partial melting of mantle wedge and evolution of island arc crust. *Journal of Geophysical Research* 95 (B10), 15929–15939. http://dx.doi.org/10.1029/JB095iB10p15929.

Kuzmichev A.B., 2004. Tectonic History of the Tuva-Mongolia Terrane: Early Baikalian, Late Baikalian, and Early Caledonain Orogenies. Probel-2000, Moscow, 192 p. (in Russian) [*Кузьмичев А.Б.* Тектоническая история Тувино-Монгольского массива: раннебайкальский, позднебайкальский и раннекаледонский этапы. М.: Пробел-2000, 2004. 192 с.].

Langmuir C.H., Klein E.M., Plank, T., 1992. Petrological systematics of mid-ocean ridge basalts: constraints on melt generation beneath ocean ridges. In: J.P. Morgan, D.K. Blackman, J.M. Sinton (Eds.), Mantle Flow and Melt Generation at Mid-Ocean Ridges. AGU Geophysical Monograph Series, vol. 71, p. 183–280. http://dx.doi.org/10.1029/GM071p0183.

Larson R.L., 1991. Geological consequences of superplumes. *Geology* 19 (10), 963–966. http://dx.doi.org/10.1130/0091-7613(1991)019<0963:GCOS>2.3.CO;2.

Le Bas M.J., 2000. IUGS reclassification of the high-Mg and picritic volcanic rocks. *Journal of Petrology* 41 (10), 1467–1470. http://dx.doi.org/10.1093/petrology/41.10.1467.

Leybourne M.I., van Wagover N.A., Ayers L.D., 1997. Chemical stratigraphy and petrogenesis of Early Proterozoic Amisk Lake volcanic sequence, Flin Flon-Snow Lake greenstone belt, Canada. *Journal of Petrology* 38 (11), 1541–1564. http://dx.doi.org/10.1093/petroj/38.11.1541.

Li Y.-B., Kimura J.-I., Machida S., Ishii T., Ishiwata A., Maruyama S., Qiu H.-N., Ishikawa T., Kato Y., Haraguchi S., Takahata N., Hirahara Y., Miyazaki T., 2013. High-Mg adakite and low-Ca boninite from a Bonin fore-arc seamount: Implications for the reaction between slab melts and depleted mantle. *Journal of Petrology* 54 (6), 1149–1175. http://dx.doi.org/10.1093/petrology/egt008.

Macpherson C.G., Hall R., 2001. Tectonic setting of Eocene boninite magmatism in the Izu-Bonin-Mariana forearc. *Earth and Planetary Science Letters* 186 (2), 215–230. http://dx.doi.org/10.1016/S0012-821X(01)00248-5.

Manikyamba C., Kerrich R., 2012. Eastern Dharwar Craton, India: continental lithosphere growth by accretion of diverse plume and arc terranes. *Geoscience Frontiers* 3 (3), 225–240. http://dx.doi.org/10.1016/j.gsf.2011.11.009.

Manikyamba C., Naqvi S.M., Subba Rao D.V., Ram Mohan M., Khanna Tarun C., Rao T.G., Reddy G.L.N., 2005. Boninites from the Neoarchaean Gadwal Greenstone belt, Eastern Dharwar Craton, India: implications for Archaean subduction processes. *Earth and Planetary Science Letters* 230 (1–2), 65–83. http://dx.doi.org/10.1016/j.epsl.2004.06.023.

Manikyamba C., Ray J., Ganguly S., Singh M.R., Santosh M., Saha A., Satyanarayanan M., 2015. Boninitic metavolcanic rocks and island arc tholeiites from the Older Metamorphic Group (OMG) of Singhbhum Craton, eastern India: Geochemical evidence for Archean subduction processes. *Precambrian Research* 271, 138–159. http://dx.doi.org/10.1016/j.precamres.2015.09.028.

Martin E., Martin H., Sigmarsson O., 2008. Could Iceland be a modern analogue for the Earth's early continental crust? *Terra Nova* 20 (6), 463–468. http://dx.doi.org/10.1111/j.1365-3121.2008.00839.x.

Meffre S., Aitchison J.C., Crawford A. J., 1996. Geochemical evolution and tectonic significance of boninites and tholeiites from the Koh ophiolite, New Caledonia. *Tectonics* 15 (1), 67–83. http://dx.doi.org/10.1029/95TC02316.

Metcalf R.V., Shervais J.W., 2008. Suprasubduction-zone ophiolites: Is there really an ophiolite conundrum? In: J.E. Wright, J.W. Shervais (Eds.), Ophiolites, arcs, and batholiths: A tribute to Cliff Hopson. Geological Society of America Special Papers, vol. 438, p. 191–222. http://dx.doi.org/10.1130/2008.2438(07).

Miyashiro A., 1973. The Troodos ophiolitic complex was probably formed in an island arc. *Earth and Planetary Science Letters* 19 (2), 218–224. http://dx.doi.org/10.1016/0012-821X(73)90118-0.

Molina J.F., Poli S., 2000. Carbonate stability and fluid composition in subducted oceanic crust: an experimental study on H_2O–CO_2-bearing basalts. *Earth and Planetary Science Letters* 176 (3), 295–310. http://dx.doi.org/10.1016/S0012-821X(00)00021-2.

Natland J.H., 1981. Crystal morphologies and pyroxene compositions in boninites and tholeiitic basalts from Deep Sea Drilling Project Holes 458 and 459B in the Mariana fore-arc region. In: Initial reports of the Deep Sea Drilling Project, vol. 60, p. 681–707.

Niu Y., O'Hara M.J., 2009. MORB mantle hosts the missing Eu (Sr, Nb, Ta and Ti) in the continental crust: New perspectives on crustal growth, crust–mantle differentiation and chemical structure of oceanic upper mantle. *Lithos* 112 (1–2), 1–17. http://dx.doi.org/10.1016/j.lithos.2008.12.009.

Niu Y., O'Hara M.J., Pearce J.A., 2003. Initiation of subduction zones as a consequence of lateral compositional buoyancy contrast within the lithosphere: a petrological perspective. *Journal of Petrology* 44 (5), 851–866. http://dx.doi.org/10.1093/petrology/44.5.851.

O'Hara M.J., Herzberg C., 2002. Interpretation of trace element and isotope features of basalts: relevance of field relations, petrology, major element data, phase equilibria, and magma chamber modeling in basalt petrogenesis. *Geochimica et Cosmochimica Acta* 66 (12), 2167–2191. http://dx.doi.org/10.1016/S0016-7037(02)00852-9.

Pagé P., Bédard J.H., Tremblay A., 2009. Geochemical variations in a depleted fore-arc mantle: The Ordovician Thetford Mines Ophiolite. *Lithos* 113 (1–2), 21–47. http://dx.doi.org/10.1016/j.lithos.2009.03.030.

Palmeri R., Sandori S., Godard G., Ricci C.A., 2012. Boninite-derived amphibolites from the Lanterman-Mariner suture (northern Victoria Land): New geochemical and petrological data. *Lithos* 140–141, 200–223. http://dx.doi.org/10.1016/j.lithos.2012.02.001.

Pearce J.A., 1982. Trace element characteristics of lavas from distinctive plate boundaries. In: J. Thorpe (Ed.), Andesites. John Wiley, New York, p. 525–548.

Pearce J.A., 2003. Supra-subduction zone ophiolites: The search for modern analogues. In: Y. Dylek, S. Newcomb (Eds.), Ophiolite concept and the evolution of geological thought. Geological Society of America Special Papers, vol. 373, p. 269–293. http://dx.doi.org/10.1130/0-8137-2373-6.269.

Pearce J.A., 2008. Geochemical fingerprinting of oceanic basalts with applications to ophiolite classification and the search for Archean oceanic crust. *Lithos* 100 (1–4), 14–48. http://dx.doi.org/10.1016/j.lithos.2007.06.016.

Pearce J.A., Ernewein M., Bloomer S.H., Parson L.M., Murton B.J., Johnson L.E., 1994. Geochemistry of Lau Basin volcanic rocks: influence of ridge segmentation and arc proximity. In: J.L. Smellie (Ed.), Volcanism associated with extension at consuming plate margins. Geological Society, London, Special Publications, vol. 81, 53–75. http://dx.doi.org/10.1144/GSL.SP.1994.081.01.04.

Pearce J.A., Lippard S.J., Roberts S., 1984. Characteristics and tectonic significance of supra-subduction zone ophiolites. In: B.P. Kokelaar, M.F. Howells (Eds.), Marginal basin geology: volcanic and associated sedimentary and tectonic processes in modern and ancient arginal basins. Geological Society, London, Special Publications, vol. 16, p. 77–94. http://dx.doi.org/10.1144/GSL.SP.1984.016.01.06.

Pearce J.A., Robinson P.T., 2010. The Troodos ophiolitic complex probably formed in a subduction initiation, slab edge setting. *Gondwana Research* 18 (1), 60–81. http://dx.doi.org/10.1016/j.gr.2009.12.003.

Pearce J.A., van der Laan S.R., Arculus R.J., Murton B.J., Ishii T., Peate D.W., Parkinson I.J., 1992. Boninite and harzburgite from leg 125 (Bonin-Mariana forearc): a case study of magma genesis during the initial stages of subduction. In: P. Fryer, P. Coleman, J.A. Pearce, L.B. Stokking (Eds.), Proceedings of the Ocean Drilling Program, Scientific Results, vol. 125, p. 623–658. http://dx.doi.org/10.2973/odp.proc.sr.125.172.1992.

Pe-Piper G., Tsikouras B., Hatzipanagiotou K., 2004. Evolution of boninites and island-arc tholeiites in the Pindos Ophiolite, Greece. *Geological Magazine* 141 (4), 455–469. http://dx.doi.org/10.1017/S0016756804009215.

Piercey S.J., Murphy D.C., Mortensen J.K., Paradis S., 2001. Boninitic magmatism in a continental margin setting: Yukon-Tanana terrane, southeastern Yukon, Canada. *Geology* 29 (8), 731–734. http://dx.doi.org/10.1130/0091-7613(2001)029<0731:BMIACM>2.0.CO;2.

Poidevin J.-L., 1994. Boninite-like rocks from the Palaeoproterozoic greenstone belt of Bogoin, Central African Republic: Geochemistry and petrogenesis. *Precambrian Research* 68 (1–2), 97–113. http://dx.doi.org/10.1016/0301-9268(94)90067-1.

Polat A., Hofmann A.W., 2003. Alteration and geochemical patterns in the 3.7–3.8 Ga Isua greenstone belt. *Precambrian Research* 126 (3–4), 197–218. http://dx.doi.org/10.1016/S0301-9268(03)00095-0.

Polat A., Hofmann A.W., Rosing M.T., 2002. Boninite-like volcanic rocks in the 3.7–3.8 Ga Isua greenstone belt, West Greenland: geochemical evidence for intra-oceanic subduction zone processes in the early Earth. *Chemical Geology* 184 (3–4), 231–254. http://dx.doi.org/10.1016/S0009-2541(01)00363-1.

Puchkov V.N., 2010. Geology of the Urals and Cis-Urals (actual problems of stratigraphy, tectonics, geodynamics and metallogeny). DesignPoligraphService Publ., Ufa, 280 p. (in Russian) [*Пучков В.Н.* Геология Урала и Приуралья (актуальные вопросы стратиграфии, тектоники, геодинамики и металлогении). Уфа: ДизайнПолиграф Сервис, 2010. 280 с.].

Puchtel I.S., Hofmann A.W., Mezger K., Jochum K.P., Shchipansky A.A., Samsonov A.V., 1998. Oceanic plateau model for continental crustal growth in the Archaean: a case study from the Kostomuksha greenstone belt, NW Baltic Shield. *Earth and Planetary Science Letters* 155 (1–2), 57–74. http://dx.doi.org/10.1016/S0012-821X(97)00202-1.

Resing J.A., Rubin K.H., Embley R.W., Lipton J.H., Baker E.T., Dziak R.P., Baumberger T., Lilley M.D., Huber J.A., Shank T.M., Butterfield D.A., Clague D.A., Keller N.S., Merle S.G., Buck N.J., Michael P.J., Soule A., Caress D.W., Walker S.L., Davis R., Cowen J.P., Reysenbach A.-L., Tomas H., 2011. Active submarine eruption of boninite in the northeastern Lau Basin. *Nature Geoscience* 4 (11), 799–806. http://dx.doi.org/10.1038/ngeo1275.

Rogers G., Saunders A.D., 1989. Magnesian andesites from Mexico, Chile and the Aleutian Islands: implications for magmatism associated with ridge-trench collision. In: A. Crawford (Ed.), Boninites and related rocks. Unwin Hyman, London, p. 416–445.

Rosen O.M., Shchipansky A.A., Turkina O.M., 2008. Early Earth Geodynamics: Stability vs. Evolution in Geological Processes. Nauchny Mir, Moscow, 184 p. (in Russian) [*Розен О.М., Щипанский А.А., Туркина О.М.* Геодинамика ранней Земли: эволюция и устойчивость геологических процессов. М.: Научный мир, 2008. 184 с.].

Shchipansky A.A., 2008. Subduction vs. Mantle Plume processes in Geodynamics of Archean Greenstone Belts. LIK, Moscow, 560 p. (in Russian) [*Щипанский А.А.* Субдукционные и мантийно-плюмовые процессы в геодинамике формирования архейских зеленокаменных поясов. М.: Изд-во ЛИК, 2008. 560 с.].

Shchipansky A.A., 2012. Subduction geodynamics in Archean and formation of diamond-bearing lithospheric keels and early continental crust of cratons. *Geotectonics* 46 (2), 122–141. http://dx.doi.org/10.1134/S0016852112020057.

Shchipansky A.A., Babarina I.I., Krylov K.A., Samsonov A.V., Bogina M.M., Bibikova E.V., Slabunov A.I., 2001. The oldest ophiolites: the late Archean suprasubduction zone complex of the Iringora structure, North Karelian greenstone belt. *Doklady Earth Science* 377A (3), 283–287.

Shchipansky A.A., Samsonov A.V., Bibikova E.V., Babarina I.I., Krylov K.A., Konilov A.N., Slabunov A.I., Bogina M.M., 2004. 2.8 Ga boninite-hosting partial suprasubduction zone ophiolite sequences from the North Karelian greenstone belt, NE Baltic Shield, Russia. In: T. Kusky (Ed.), Precambrian ophiolites and related rocks. Elsevier, Amsterdam, p. 424–486. http://dx.doi.org/10.1016/S0166-2635(04)13014-4.

Shchipansky A.A., Samsonov A.V., Bogina M.M., Slabunov A.I., Bibikova E.V., 1999. High-Mg, low-Ti quartz amphibolites of the Khizovaara greenstone belt, Northern Karelia: Archean metamorphosed boninites? *Doklady Earth Science* 365A (3), 422–425.

Shervais J.W., 2001. Birth, death, and ressurection: The life cycle of of suprasubduction zone ophiolites. *Geochemistry, Geophysics, Geosystems* 2 (1), 1010. http://dx.doi.org/10.1029/2000GC000080.

Shervais J.W., Kimbrough D.L., Renne P.R., Hanan B.B., Murchey B., Snow C.A., Zoglman-Schuman M.M., Beaman J., 2004. Multi-stage origin of the Coast Range ophiolite, California: Implications for the life cycle of supra-subduction zone ophiolites. *International Geology Review* 46 (4), 289–315. http://dx.doi.org/10.2747/0020-6814.46.4.289.

Shervais J.W., Murchey B., Kimbrough D.L., Renne P.R., Hanan B.B., 2005. Radioisotopic and biostratigraphic age relations in the Coast Range Ophiolite, northern California: Implications for the tectonic evolution of the Western Cordillera. *Geological Society of America Bulletin* 117 (5–6), 633–653. http://dx.doi.org/10.1130/B25443.1.

Shi R., Yang J., Xu Z., Oi X., 2004. Discovery of the boninite series volcanic rocks in the Bangong Lake ophiolite mélange, western Tibet, and its tectonic implications. *Chinese Science Bulletin* 49 (12), 1272–1278. http://dx.doi.org/10.1360/04wd0006.

Shi R., Yang J., Xu Z., Oi X., 2008. The Bangong Lake ophiolite (NW Tibet) and its bearing on the tectonic evolution of the Bangong-Nujiang suture zone. *Journal of Asian Earth Sciences* 32 (5), 438–457. http://dx.doi.org/10.1016/j.jseaes.2007.11.011.

Simonov V.A., Dobretsov N.L., Buslov M.M., 1994. Boninite series in structures of the Paleo-Asian Ocean. *Geologiya i Geofizika* (*Russian Geology and Geophysics*) 35 (7–8), 182–199 (in Russian) [*Симонов В.А., Добрецов Н.Л., Буслов М.М.* Бонинитовые серии в структурах Палеоазиатского океана // *Геология и геофизика*. 1994. Т. 35. № 7–8. С. 182–199].

Simonov V.A., Safonova I.Y., Kovyazin S.V., 2010. Petrogenesis of the island-arc complexes of the Chara zone, East Kazakhstan. *Petrology* 18 (6), 610–623. http://dx.doi.org/10.1134/S0869591110060044.

Sklyarov E.V., Kovach V.P., Kotov A.B., Kuzmichev A.B., Lavrenchuk A.V., Perelyaev V.I., Shchipansky A.A., 2016. Boninites and ophiolites: Problems of their relations and petrogenesis of boninites. *Russian Geology and Geophysics* 57 (1), 127–140. http://dx.doi.org/10.1016/j.rgg.2016.01.009.

Sleep N.H., 1992. Archean plate tectonics: what can be learned from continental geology? *Canadian Journal of Earth Sciences* 29 (10), 2066–2071. http://dx.doi.org/10.1139/e92-164.

Smellie J.L., Stone P., Evans J., 1995. Petrogenesis of boninites in the Ordovician Ballantrae Complex ophiolite, southwestern Scotland. *Journal of Volcanology and Geothermal Research* 69 (3–4), 323–342. http://dx.doi.org/10.1016/0377-0273(95)00037-2.

Sobolev A.V., Danyushevsky L.V., 1994. Petrology and geochemistry of boninites from the north termination of the Tonga trench: constraints on the generation conditions of primary high-Ca boninite magmas. *Journal of Petrology* 35 (5), 1183–1211. http://dx.doi.org/10.1093/petrology/35.5.1183.

Sobolev A.V., Portnyagin M.V., Dmitriev L.V., Tsameryan O.P., Danyushevsky L.V., Kononkova N.N., Schimizu N., Robinson P.T., 1993. Petrology of ultramafic lavas and associated rocks of the Troodos Massif, Cyprus. *Petrologiya* (*Petrology*) 1 (4), 331–361 (in Russian) [*Соболев А.В., Портнягин М.В., Дмитриев Л.В., Цамерян О.П., Данюшевский Л.В., Кононкова Н.Н., Шимизу Н., Робинсон П.Т.* Петрология ультрамафических лав и связанных с ними пород массива Троодос, о-в Кипр // *Петрология*. 1993. Т. 1. № 4. С. 331–361].

Spadea P., Kabanova L.Y., Scarrow J.H., 1998. Petrology, geochemistry and geodynamic significance of Mid-Devonian boninitic rocks from the Baimak-Buribai area (Magnitogorsk Zone, southern Urals). *Ofioliti* 23, 17–36.

Stern R.A., Syme E.C., Bailes A.Y., Lukas S.B., 1995. Paleoproterozoic (1.90–1.86 Ga) arc volcanism in the Flin Flon Belt, Trans-Yudson orogen, Canada. *Contributions to Mineralogy and Petrology* 119 (2), 117–141. http://dx.doi.org/10.1007/BF00307276.

Stern R.J., 2002. Subduction zones. *Reviews of Geophysics* 40 (4), 1012. http://dx.doi.org/10.1029/2001RG000108.

Stern R.J., 2004. Subduction initiation: spontaneous and induced. *Earth and Planetary Science Letters* 226 (3–4), 275–292. http://dx.doi.org/10.1016/j.epsl.2004.08.007.

Stern R.J., Bloomer S.H., 1992. Subduction zone infancy: Examples from the Eocene Izu-Bonin-Mariana and Jurassic California arcs. *Geological Society of America Bulletin* 104 (12), 1621–1636. http://dx.doi.org/10.1130/0016-7606(1992)104<1621:SZIEFT>2.3.CO;2.

Stern R.J., Morris J., Bloomer S.H., Hawkins J.W., 1991. The source of the subduction component in convergent margin magmas: trace element and radiogenic evidence from Eocene boninites, Mariana forearc. *Geochimica et Cosmochimica Acta* 55 (5), 1467–1481. http://dx.doi.org/10.1016/0016-7037(91)90321-U.

Sun S.-S., Nesbitt R.W., 1978. Geochemical regularities and genetic significance of ophiolitic basalts. *Geology* 6 (11), 689–693. http://dx.doi.org/10.1130/0091-7613(1978)6<689:GRAGSO>2.0.CO;2.

Tatsumi Y., Ishizaka K., 1981. Existence of andesitic primary magma: an example from Southwest Japan. *Earth and Planetary Science Letters* 53 (1), 124–130. http://dx.doi.org/10.1016/0012-821X(81)90033-9.

Taylor R.N., Nesbitt R.W., 1998. Isotopic characteristics of subduction fluids in an intra-oceanic setting, Izu-Bonin Arc, Japan. *Earth and Planetary Science Letters* 164 (1–2), 79–98. http://dx.doi.org/10.1016/S0012-821X(98)00182-4.

Taylor R.N., Nesbitt R.W., Vidal P., Harmon R.S., Auvray B., Croudace I.W., 1994. Mineralogy, and genesis of the boninite series volcanics, Chichijima, Bonin Island, Japan. *Journal of Petrology* 35 (3), 577–617. http://dx.doi.org/10.1093/petrology/35.3.577.

Turner S., Hawkesworth C., 1997. Constraints on flux rates and mantle dynamics beneath island arcs from Tonga-Kermadec lava geochemistry. *Nature* 389 (6651), 568–573. http://dx.doi.org/10.1038/39257.

Van de Zedde D.M.A., Wortel M.J.R., 2001. Shallow slab detachment as a transient source of heat at midlithospheric depths. *Tectonics* 20 (6), 868–882. http://dx.doi.org/10.1029/2001TC900018.

Walker D.A., Cameron W.E., 1983. Boninite primary magmas: evidence from the Cape Vogel Peninsula. *Contributions to Mineralogy and Petrology* 83 (1), 150–158. http://dx.doi.org/10.1007/BF00373088.

Walker D., Shibata T., De Long S.E., 1979. Abyssal tholeiites from the Oceanographer Fracture Zone. II. Phase equilibria and mixing. *Contributions to Mineralogy and Petrology* 70 (2), 111–125. http://dx.doi.org/10.1007/BF00374440.

Wallin E.T., Metcalf. R.V., 1998. Supra-subduction zone ophiolite formed in an extensional forearc: Trinity Terrane, Klamath Mountains, California. *The Journal of Geology* 106 (5), 591–608. http://dx.doi.org/10.1086/516044.

Whattam S.A., Stern R.J., 2011. The 'subduction initiation rule': a key for linking ophiolite, intra-oceanic forearcs, and subduction initiation. *Contributions to Mineralogy and Petrology* 162 (5), 1031–1045. http://dx.doi.org/10.1007/s00410-011-0638-z.

Wolde B., Asres Z., Desta Z., Gonzalez J.J., 1996. Neoproterozoic zirconium-depleted boninite and tholeiite series rocks from Adola, southern Ethiopia. *Precambrian Research* 80 (3), 261–279. http://dx.doi.org/10.1016/S0301-9268(96)00018-6.

Wyman D.A., 1999a. A 2.7 Ga depleted tholeiite suite: evidence of plume-arc interaction in the Abitibi greenstone belt, Canada. *Precambrian Research* 97 (1–2), 27–42. http://dx.doi.org/10.1016/S0301-9268(99)00018-2.

Wyman D.A., 1999b. Paleoproterozoic boninites in an ophiolite-like setting, Trans-Hudson orogen, Canada. *Geology* 27 (5), 455–458. http://dx.doi.org/10.1130/0091-7613(1999)027<0455:PBIAOL>2.3.CO;2.

Wyman D.A., Kerrich R., Groves D.I., 1999. Lode gold deposits and Archean mantle-plume island arc interaction, Abitibi Subprovince, Canada. *The Journal of Geology* 107 (6), 715–725. http://dx.doi.org/10.1086/314376.

Xia X., Song S., Niu Y., 2012. Tholeiite–boninite terrane in the North Qilian suture zone: Implications for subduction initiation and back-arc basin development. *Chemical Geology* 328, 259–277. http://dx.doi.org/10.1016/j.chemgeo.2011.12.001.

Yibas B., Reimold W.U., Anhaeusser C.R., Koeberl C., 2003. Geochemistry of the mafic rocks of the ophiolitic fold and thrust belts of southern Ethiopia: constraints on the tectonic regime during the Neoproterozoic (900–700 Ma). *Precambrian Research* 121 (3–4), 157–183. http://dx.doi.org/10.1016/S0301-9268(02)00197-3.

Yumul G.P., 1996. Varying mantle sources of supra-subduction zone ophiolites: REE evidence from the Zambales Ophiolite Complex, Luzon, Philippines. *Tectonophysics* 262 (1–4), 243–262. http://dx.doi.org/10.1016/0040-1951(96)00013-3.

Yumul Jr G.P., Dimalanta C.B., Jumawan F.T., 2000. Geology of the southern Zambales Ophiolite Complex, Luzon, Philippines. *Island Arc* 9 (4), 542–555. http://dx.doi.org/10.1111/j.1440-1738.2000.00300.x.

Zhao J.-H., Asimov P.D., 2014. Neoproterozoic boninite-series rocks in South China: A depleted mantle source modified by sediment-derived melt. *Chemical Geology* 388, 98–111. http://dx.doi.org/10.1016/j.chemgeo.2014.09.004.

Zonenshain L.P., Kuzmin M.I., 1978. Khantaishir ophiolite complex in western Mongolia and ophiolite problem. *Geotektonika* (*Geotectonics*) (1), 19–42 (in Russian) [*Зоненшайн Л.П., Кузьмин М.И.* Хантайширский офиолитовый комплекс Западной Монголии и проблема офиолитов // *Геотектоника*. 1978. № 1. С. 19–42].

Shchipansky, Andrei A., Doctor of Geology and Mineralogy, Lead Researcher
Geological Institute of RAS
7 Pyzhevsky lane, Moscow 119017, Russia
✉ e-mail: shchipansky@mail.ru

Щипанский Андрей Анатольевич, докт. геол.-мин. наук, в.н.с.
Геологический институт РАН
119017, Москва, Пыжевский пер., 7, Россия
✉ e-mail: shchipansky@mail.ru